1   **Stratigraphic architecture and hierarchy of fluvial overbank splay deposits**

2   C.E. Burns*, N.P. Mountney, D.M. Hodgson, L. Colombera

3   *Fluvial & Eolian Research Group, School of Earth and Environment, University of Leeds,*

4   *Leeds, LS2 9JT, UK*

5   *Correspondence (catherineburns91@gmail.com)*

6   **Abstract**

7   Splay deposits represent an important sand-prone component of the otherwise fine-grained

8   stratigraphic record of fluvial overbank systems. This work presents a hierarchical approach

9   to the classification and palaeoenvironmental interpretation of ancient preserved splay

10   deposits supported by the analysis of the stratigraphic architecture of eleven exhumed

11   examples from the Jurassic Morrison Formation and the Cretaceous Mesaverde Group

12   (Western USA) and analysis of the morphology of splays from nine modern fluvial systems. A

13   hierarchical arrangement of splay deposits is proposed, categorised into lithofacies, beds,

14   elements and complexes. Recognition criteria for each tier of the hierarchy include

15   identification of bounding surfaces, thinning and fining trends of splay elements and

16   complexes, and palaeocurrent variability. Progradational and compensational stacking

17   trends control the stratal architecture of splay deposits, and these are influenced by the

18   following factors: (i) the rate of local accommodation generation, which influences the

19   erosive power of floodwaters and whether splay elements are laterally offset due to

20   compensational stacking; (ii) the nature of the topographic confinement of the floodplain;

21   and (iii) the preservation potential linked to migration direction of channel.

22   Splay bodies can contribute volume to fluvial reservoirs and may form significant connectors

23   that link otherwise isolated primary channel bodies, thereby enhancing reservoir

24   connectivity.

25

26

27

28

29   It has long been recognised that fluvial sedimentary successions can be divided into stratal

30   packages bounded by a hierarchy of surfaces (Allen 1983; Miall 1985; Bridge 1993, 2006).

31   Although overbank successions are recognised in most fluvial hierarchical schemes (Allen

32   1983; Miall 1985; Holbrook 2001; Colombera *et al.* 2013; Ford & Pyles 2014; Miall 2014),

33   relatively limited research has been undertaken previously to evaluate how overbank

34   sediments are organised stratigraphically (Fielding 1984; Bridge 1984; Jorgensen & Fielding

35   1996; Demko *et al.* 2004; Toonen *et al.* 2015). This is despite extensive work having been

36   undertaken to show how floodplains are constructed in modern systems (e.g. Farrell 1987;

37   Smith *et al.* 1989; Nanson & Croke 1992; Morozova & Smith 2000).

38   The aim of this work is to understand the mechanisms by which fluvial splay deposits

39   accumulate and become preserved in the stratigraphic record through lateral and vertical

40   stacking of multiple flood-related deposits at a hierarchy of different scales. Specific

41   research objectives are: (i) to establish recognition criteria to be used in a novel hierarchy

42   scheme for aiding identification of different sediment bodies that comprise fluvial overbank

43   successions; (ii) to evaluate outcrop data using facies and architectural-element analysis to

44   recognise the proposed hierarchical classification scheme for splay deposits; (iii) to identify

45   the different stacking patterns of splay deposits; and (iv) to discuss the wider applicability of

46   the hierarchical grouping for the development of a generic classification scheme for

47   overbank successions.

48

49   **Background**

50   Fluvial floodplains receive channel-derived sediment via overbank flooding, either by levee

51   over-topping (Fisher *et al.* 2008) or by breakout through the levees and the formation of

52   crevasse channels and splays (Ethridge, *et al.* 1999; Shen *et al.* 2015). The scale and

53   geometry of splay deposits are thought to result from an interplay of factors, including

54   parent-river size, grain-size and dominant mode of sediment transport, levee development,

55   flood characteristics and timing, and floodplain drainage (Pizzuto 1987; Williams 1989;

56   Parker 1991; Cazanacli & Smith 1998; Adams *et al.* 2004; Gulliford *et al.* 2017; Millard *et al.*

57   2017).

58   The size of a parent river is a first-order control on splay size, whereby larger rivers

59   associated with greater water discharge typically have available a larger volume of sediment

60   for potential supply onto the floodplain (Williams 1989). However, other factors are also

61   known to play an important role in splay development.

62   Floodplain morphology and drainage will have an important impact on the spatial

63   distribution of splay sedimentation; the water-surface slope — i.e., the difference between

64   the water level in the river and the floodplain water level, which usually decreases away

65   from the main channel, influences the deposition rates away from the crevasse-splay

66   breakout point (Pizzuto 1987; Adams *et al.* 2004; Millard *et al.* 2017). The water-surface

67   slope tends to increase in accord with the channel water level during a flooding event,

68   thereby driving sediment transport onto the floodplain (Adams *et al.* 2004; Millard *et al.*

69   2017).

70   The grain size of the sediment transported through crevasse channels will influence the

71   patterns of deposition, whereby coarser sediment is preferentially deposited in a position

72   proximal to the breakout point, whereas finer sediment will be deposited farther onto the

73   floodplain (Parker 1991; Cazanacli & Smith 1998; Slingerland & Smith 1998; Fedele & Paola

74   2007; Millard *et al.* 2017). Crevasse-splays are fundamentally linked to levee development.

75   River systems with better developed levees are more likely to experience major splay-

76   producing floods as crevasse channels must cut through the levees (Brierley *et al*. 1997;

77   Florsheim & Mount 2002).

78   In contrast, floodplain deposits such as palaeosols, coals, or organic-rich rooted siltstones,

79   represent a local hiatus in splay deposition, possibly because of a shift of the river channel

80   away from the site of deposition (Slingerland & Smith 2004; van Toorenenburg *et al.* 2016).

81   As such, these types of floodplain deposits have previously been used for subdividing silt-

82   and sand-prone crevasse-splay deposits (Mjøs *et al.* 1993), and for attempting correlation

83   between stacked splay units to channel belts (Gulliford *et al*. 2017). Palaeosol profiles can

84   be used to infer the frequency of splay development. For this work, and at multiple levels of

85   the hierarchy, poor-quality, immature soil profiles occur between frequently (decadal-scale)

86   emplaced splays, whereas more mature soil profiles occur between larger splay bodies

87   whose top records a more significant temporal gap in splay deposition (Kraus 1987). In turn,

88   splay deposition hinders pedogenic processes locally within the floodplain, and prevents the

89   development of thick mature palaeosols in proximity to the parent river channel (Bown &

90   Kraus 1987; Kraus 1987; Wright & Marriott 1993; Kraus 1999). Palaeosols and coals can be

91   readily recognised in outcrop or core, and can be used as proxies for periods of reduced

92   sediment input to parts of a floodplain (Kraus 1999).

93   Stratigraphic hierarchical classification schemes are employed as a method to package and

94   divide sedimentary successions. Different genetically related packages are assigned on the

95   basis of recognition of common assemblages of one or more lithofacies that define

96   elements with distinctive geometries and which are themselves delineated by bounding

97   surfaces at a variety of scales, from lamina-scale to basin-scale (Fig. 1; Allen 1966, 1983;

98   Miall 1985, 1988). Hierarchical schemes are used widely in sedimentology from aeolian

99   settings (e.g. Brookfield 1977; Kocurek 1981) to deep-water settings (e.g. Sprague *et al.*

100   2002; Prélat *et al*. 2009). Their application to fluvial systems (e.g. Allen 1983; Friend 1983)

101   has imposed recognisable order to sedimentary successions and provides insight to

102   palaeoenvironmental setting. However, existing fluvial hierarchy schemes do not

103   differentiate effectively the various component parts of overbank successions, composed of

104   stacked splay bodies. Indeed, relatively few outcrop studies have focused specifically on the

105   facies organisation and stratal architecture of overbank and splay deposits (Bridge 1984;

106   Fielding 1984; Mjøs 1993; Demko *et al.* 2004; Ford & Pyles, 2014; Van Toorenenburg *et al*.

107   2016; Burns *et al.* 2017).

108   Splays and their associated deposits are commonly considered, perhaps simplistically, as

109   lobate bodies in plan-view and wedge-shaped in cross-sectional view (Coleman, 1969;

110   O'Brien &Wells 1986; Smith *et al.* 1989; Florsheim & Mount 2002; Arnaud-Fassetta 2013). A

111   crevasse-splay deposit is a body of sediment delivered through a breach in the channel bank

112   or levee into the adjacent overbank floodbasin (Ethridge *et al.* 1999; Shen *et al.* 2015).

113   However, not all splays are crevasse-splays. Some splays originate via overbank flooding

114   with no crevasse incision (Fisher *et al.* 2008) yet can lead to widespread splay deposition on

115   the floodplain (e.g. Coleman 1968; Jordan & Pryor 1991). In ancient successions it can be

116   difficult to identify whether a particular splay is genetically related to a particular crevassing

117   event; only rarely are genetically-related crevasse channels evident. In this work we use the

118   term 'splay' to encompass both crevasse splays and splays originating from overtopping of a

119   levee or bank by flood waters.

120   Analysis of modern fluvial systems indicates that simple lobate splays can, given sufficient

121   time and available accommodation, evolve into composite digitated forms, in some cases

122   developing anastomosing channel patterns prior to abandonment (Smith *et al.* 1989; Smith

123 & Perez-Arlucea 1994; Ethridge *et al.* 1999; Farrell 2001). Additionally, in both modern

124 systems and ancient successions, individual splay deposits or forms are seen to coalesce and

125 construct larger composite units over time (Smith *et al.* 1989; Shanley *et al.* 1992; Mjøs *et*

126 *al.* 1993; Florshein & Mount 2002); such composite units have been called 'complexes'

127 (Smith *et al.* 1989). The construction of multiple, amalgamated splay bodies, as commonly

128 recognised in modern systems, suggests that a hierarchical approach for the

129 characterisation of accumulated fluvial overbank successions is appropriate.

130

131 **Hierarchy**

132 Based on a review of published studies of the sedimentary architecture and

133 geomorphological evolution of splays (O'Brien &Wells 1986; Smith *et al.* 1989; Mjøs *et al.*

134 1993; Smith & Perez-Arlucea 1994; Jorgenson & Fielding 1996; Ethridge *et al.* 1999; Farrell

135 2001; Florsheim & Mount 2002), a hierarchical scheme that can be used for categorising the

136 deposits of splays is proposed here; the applicability of the scheme is then assessed against

137 purposely acquired field data. The lower three tiers of the hierarchy scheme are based in

138 part on the classic fluvial hierarchy by Miall (1985) but focus on the overbank and splays.

139 The uppermost tier of the hierarchy is based on studies of modern splays by workers such as

140 Smith et al. (1989), Smith & Perez-Arlucea (1994) and Florsheim & Mount (2002).

141 The first two tiers of the hierarchy proposed herein are represented by the 'lithofacies' and

142 by the 'beds' they form, which may consist of accumulations of individual lithofacies or may

143 be made up of an association of multiple lithofacies types (Fig. 1). Splay elements may

144 comprise a single lithofacies type or multiple facies types arranged into a vertical succession.

145 Individual beds can be difficult to identify within splay elements where they amalgamate

146 and are composed of similar facies types. In general, a bed records deposition from a single

147 event in this case (Fig. 1; Campbell 1967; Middelkoop & Asselman 1998; Törnqvist & Bridge

148 2002; Prélat *et al.* 2009). A splay bed can be defined as the product of a short-lived single

149 flood event or short-lived part of a longer flood event (Hackney *et al.* 2015).

150 The next level of the hierarchy proposed is the 'architectural element' (Fig. 1): elements are

151 bodies of strata composed internally of predictable arrangements of one or more lithofacies

152 and delineated by bounding surfaces that define an accumulation with specific geometrical

153 properties of three-dimensional shape and size (Miall 1985; Colombera *et al.* 2012).

154 Overbank architectural elements have a series of recognition criteria in outcrop (Allen 1966;

155 Miall 1985; Colombera *et al.* 2013): the nature of the upper and lower bounding surfaces

156 including the presence of fines (clay and silt); external and internal geometry, including any

157 thickness variations of the deposit; internal facies arrangements, including any grainsize

158 variations and any consistent facies trends; scale of the deposit, including its lateral extent

159 in orientations parallel and perpendicular to original flow. In splay elements, the recognition

160 criteria that need to be fulfilled for positive identification are the sharp (sometimes

161 erosional) base of the deposit, distinct thinning and fining trends towards the distal parts of

162 the deposit (sometimes difficult to infer due to lateral thinning and fining trends), the

163 occurrence of decimetre- to metre-thick deposits with lengths and widths that are

164 commonly hundreds of metres in extent.

165 The uppermost level of the proposed hierarchy is here termed the 'complex' (Fig 1):

166 genetically related splay and crevasse-channel-fill elements that stack together to form

167 composite elements and which intercalate or are juxtaposed with other overbank elements.

168 There are several recognition criteria for defining a splay complex in outcrop: a complex

169 must comprise two or more splay elements (although this characteristic may not be

170 recognisable distally); a complex can also exhibit overall thinning and fining trends in the

171 distal direction, i.e. away from the channel body that represents the formative river; in

172 proximal reaches complexes will have similar palaeoflow directions in each of the individual

173 splay elements. In a complex, the individual splay elements originate from a similar

174 breakout point in a river, although this is difficult to demonstrate unequivocally in the

175 majority of successions; non-related splays can overlap or build into the same floodbasin.

176 Such elements must also be constructed within the same floodbasin, in a manner that will

177 cause the elements to partially overlap vertically and laterally.

178

179 **Data and Methods**

180 Outcrop data have been collected from five sites in the Jurassic Morrison Formation of Utah

181 and Colorado, and from six sites in the Cretaceous Mesaverde Group (Castlegate and Neslen

182 formations) of Utah, USA (Fig. 2). Each of the sites were located in parts of the Castlegate,

183 Neslen and Morrison formations that offered exposures that were intersected by canyons

184 and followed ridges, enabling an attempt at 3D reconstruction of the elements present.

185   One-hundred-and-four graphic log sections (1,241 m cumulative length) were measured

186   from the eleven sites: forty-two in the Morrison Formation and sixty-two in the Mesaverde

187   Group. The logs record lithology, grain size, sedimentary structures, occurrence of fossils

188   and pedogenic features. Rooting and bioturbation indices were recorded on a scale from 0

189   (no rooting or bioturbation) to 5 (heavily rooted throughout with large [>10 mm] rhizoliths

190   as well as smaller root traces throughout, or intense bioturbation that masks or obliterates

191   all original primary sedimentary structures) (cf. Taylor & Goldring 1993). Sixty-seven splay

192   elements were characterised in detail, across several logged sections at each locality; eleven

193   splay complexes were recognised — four in the Morrison Formation and seven in the Neslen

194   Formation. The number of palaeocurrents measured in each splay element depends on the

195   occurrence of facies types containing palaeoflow indicators; however, splay elements in this

196   study have a minimum of ten palaeocurrents recorded and splay complexes have ten

197   measurements per element in the complex. Herein, sixteen lithofacies types from the three

198   studied formations are recognised based on composition, grain size, sediment textural

199   characteristics and sedimentary structures (Table 1). The facies scheme used is a modified

200   and extended version of the schemes of Miall (1985) and Colombera *et al*. (2013).

201   Forty-one architectural panels and accompanying photomosaics were constructed by

202   tracing units across each outcrop cliff section; 27 architectural panels were measured from

203   the Mesaverde Group and 14 from the Morrison Formation. Panels were constructed as

204   scaled drawings using spatial measurements derived directly from outcrop and checked

205   using satellite imagery. Panels record lithofacies arrangements and distributions, and

206   external geometry of splay elements, including their bounding surfaces. Palaeocurrent

207   directions were inferred from 2,118 indicators, including cross-bedding foresets, ripple

208   cross-lamination, current ripple-forms on bedding surfaces (1,118 from the Mesaverde

209   Group and 900 from the Morrison Formation). Three literature studies of ancient outcrops

210   with splay deposits have been chosen to discuss the applicability of the criteria for

211   recognition of the proposed hierarchy. Two of these studies are from river systems that are

212   interpreted to have been subject to ephemeral discharge, and therefore to have

213   experienced markedly peaked flood hydrographs: the Huesca fan, Sariñena Formation, Ebro

214   Basin (van Toorenenburg *et al.* 2016), and the Beaufort Formation, Karoo Basin (Gulliford *et*

215   *al.* 2017), whereas one is from the deltaic deposits of the Ravenscar Group, Cleveland Basin

216 (cf. Mjøs *et al.* 1993). Observations from these studies have been used to assess the wider

217 applicability of the hierarchy scheme proposed in this work.

218 To support the hierarchical scheme presented here, additional data were collected from 9

219 modern rivers, which display splay development, through analysis using Google Earth

220 imagery: the Helodrano Mahajambe, Madagascar; the Paraná River, Argentina; the

221 Saskatchewan River, Saskatchewan; the Mississippi River, Mississippi; Niobrara River,

222 Nebraska; Rhine River, Netherlands; Volga River, Russia; Ankofia River, East Madagascar;

223 and the Saloum River, Russia. Recorded information is as follows: (i) splay lengths

224 perpendicular to parent channel at the breakout point; (ii) splay widths parallel to parent

225 channel at the breakout point; (iii) planform geometries of splays and their associated trunk-

226 channel sizes. The use of satellite imagery from modern river systems precludes comparison

227 to ancient examples in both formative processes and preserved stratigraphic expression as

228 surfaces and stratigraphic packages. In addition, the observed landforms do not record the

229 morphodynamic evolution of a crevasse splay from inception to abandonment, and might

230 not be representative of what is ultimately preserved into the long-term sedimentary

231 record. Nonetheless, these data are useful to illustrate the range of possible planform

232 morphologies of splays, and to document the relative scale of splays to their parent river

233 channels.

234

235 **Geological setting of the studied successions**

236 The Morrison Formation, Castlegate Sandstone and Neslen Formation of the Mesaverde

237 Group were chosen for study because of the well-established stratigraphic and

238 sedimentological frameworks. The Kimmeridgian Morrison Formation was deposited under

239 a semi-arid climate regime (Demko *et al.* 2004; Owen *et al.* 2015). The seasonal variations in

240 climate during deposition of the Morrison Formation were associated with a flashy

241 discharge regime (Owen *et al.* 2015). The semi-arid climate is recorded in palaeosol deposits

242 associated with drier settings (Demko *et al.* 2004). The Morrison Formation accumulated

243 within the North American Cordilleran foreland basin (Fig. 2; Decelles & Burden 1991;

244 Decelles & Currie 1996; Currie 1997). The Salt Wash Member is interpreted as a distributive

245 fluvial system (Owen *et al.* 2015), within which the proportion of overbank deposits

246 increases from apical fan areas (0%–40%) through medial (40%–70%) and to distal (>70%)

247   parts. The studied sites in this work are in medial and distal regions of the fluvial fan: Slick

248   Rock, Naturita, Atkinson Creek, Yellow Cat Canyon (medial sections), and Colorado National

249   Monument (distal section).

250   The Lower Castlegate Sandstone is generally considered to comprise the deposits of low-

251   sinuosity braided rivers (Van Wagoner *et al.*1990; Olsen *et al*. 1995: Hettinger & Kirschbaum

252   2002), with some downdip variations towards the palaeo-shoreline, whereby the system

253   changes to a shoreline-deltaic system towards present-day Colorado (Miall 1993; Hettinger

254   & Kirschbaum 2002). The two sites studied in the Castlegate Sandstone are stratigraphically

255   in the lowest part of the formation just above the Blackhawk Formation.

256   The Neslen Formation was also deposited in the North American Cordilleran foreland basin

257   during the Late Campanian, under a persistent wet-humid climate (Huber *et al.* 2002).

258   Inferred monsoonal conditions during the Campanian (Fricke *et al.* 2010) are thought to

259   have resulted in large-scale precipitation events (Miller *et al.* 2013). The Neslen Formation

260   was deposited as part of a low-gradient, low-relief fluvial and coastal plain (Pitman *et al.*

261   1987; Lawton 1994), delta plain (Karaman 2012; O'Brien 2015; Gates & Scheetz 2015;

262   Burton *et al.* 2016; Shiers *et al.* 2017), or estuarine complex (Willis 2000; Kirschbaum &

263   Hettinger 2004; Cole 2008). Overall, there is a general coarsening-upwards trend within the

264   Neslen Formation, which can be linked to progradation from lower coastal plain, to upper

265   coastal plain, to a lower alluvial-plain setting (Franczyk *et al.* 1990; Hettinger & Kirschbaum

266   2002). The Neslen Formation can be broadly split into three zones: the Palisade zone, the

267   Ballard zone and the Chesterfield zone, each of which is delineated by sandstone marker

268   beds, and on the basis of variations in the characteristics of channelized elements and in the

269   amount of coal (Shiers *et al.* 2014; 2017). Of the four sites studied in the Neslen Formation,

270   two are within the Palisade zone (Tuscher Canyon), and two are within the Chesterfield zone

271   (Crescent Canyon).

272

273   **Recognition of the proposed hierarchy**

274   ***Lithofacies and beds***

275   Lithofacies are units with defined sediment texture and structure and represent the most

276   fundamental building block recognised in the hierarchical scheme (Fig. 1; Table 1). Facies

277   occur in genetically related associations, commonly in arrangements whereby vertical or

9

278 lateral successions of facies occur in a predictable order (cf. Walker & James 1992). Such

279 facies associations are characteristic of splay deposits (Fig. 1; Burns *et al.* 2017). A single bed

280 is composed of one or more lithofacies in vertical section and could represent a single splay

281 element (Fig. 3A). In the studied successions, all the splays made of a single bed exhibit

282 lateral thinning and fining trends, in which relatively coarser-grained facies dominate in

283 proximal parts and transition distally into finer grained facies of the medial and distal areas

284 (Fig 3B; Burns *et al.* 2017). Each of these single beds represents a single flood event

285 (Hackney *et al.* 2015).

286 Alternatively, several beds may collectively represent a coset with multiple lithofacies in

287 vertical section that have a genetically related significance (Fig. 3B). These vertical

288 successions show either a fining-upward trend or fairly constant grain size, and also exhibit

289 lateral thinning and fining trends as single-bed splays (Fig. 3B; Burns *et al.* 2017). Each bed

290 within the coset also tends to exhibit the same lateral thinning and fining trends (Fig. 3C).

291 The boundaries between these beds are sometime gradational, which renders it difficult to

292 identify separate beds, particularly when deformed facies are present. Each bed in the coset

293 could represent multiple peaks of a hydrograph or just autogenic compensation during a

294 single flood (Hackney *et al.* 2015); beds produced by these short-lived flood events stack

295 together to form the splay element.

296 Of these different splay architectures, splays made of single beds are the most common

297 across all studied successions (70.6% Morrison, 70.8% Castlegate, 59.6% Neslen; fining-

298 upwards associations are the second most common assemblage and are slightly more

299 common in the Neslen Formation than the other formations (27.8% Morrison, 10.4%

300 Castlegate, 37.5% Neslen); bed sets with constant grain size are the least common

301 architecture (1.6% Morrison, 18.8% Castlegate, 2.9% Neslen) (Fig. 3A).

302 ***Overbank elements***

303 The next level recognised in the hierarchy is the element (Fig. 1). Four overbank elements

304 are defined: splay, crevasse-channel, and floodplain and coal-prone floodplain.

305 *Splay element (CS)*

306 Bounding surfaces are the most consistent criterion for defining splay elements. The bases

307 of splay elements are sharp and can be erosional with gutter casts. The tops of splay

308 deposits, if preserved, exhibit sharp transitions to the overlying fine-grained floodplain

309   units, laminated, organic-rich rooted siltstone, coal or palaeosols (Fig. 4). Splay elements can

310   be bound at base and top by variably organic, laminated floodplain fine deposits and

311   palaeosols, which indicate a cessation of active splay deposition. Alternatively, the upper

312   parts of previously accumulated splay deposits may be eroded by the emplacement of

313   subsequent splays. Splay elements almost always thin in a downstream direction (Figs 4 & 5)

314   across all the studied formations.

315   Internal facies arrangements, including lateral facies transitions within an element, can be

316   used as a recognition criterion for splay elements. In a proximal-to-distal direction from the

317   point source, a series of predicable facies transitions is common: relatively sand-prone

318   structureless sandstone (Sm) and ripple-cross laminated sandstone (Sr) passes distally to

319   more silt-prone facies, including deformed sandstones and siltstones (Sd), and poorly sorted

320   siltstone (Fd) (Fig. 5). The most common facies within the exhumed splay elements are

321   structureless sandstone (Sm) (21% Morrison, 18% Neslen), ripple-laminated sandstone (Sr)

322   (15% Morrison, 32% Castlegate, 13% Neslen), soft-sediment deformed siltstones (Fd) (42%

323   Morrison, 21% Castlegate, 23% Neslen) and poorly sorted siltstones (Fp) (22% Morrison,

324   21% Castlegate, 36% Neslen) (Fig. 5).

325   Recognition of splay elements in fluvial overbank deposits can be aided by determination of

326   the dimensions of splay elements and their relationships with other elements. Scale

327   provides a useful indicator to establish a splay origin for deposits, but only once bounding

328   surfaces, internal facies arrangements and external geometries have been identified. Splay

329   elements reported from the ancient examples of this study have average widths (strike of

330   the deposit perpendicular to palaeoflow direction) of 672 m (71 m to 1,503 m, n=17),

331   average lengths (along dip sections that are parallel with palaeoflow directions) of 386 m

332   (94 m to 750 m, n=15) and average thickness of 1 m (0.1 m to 2.6 m, n=74) (Fig. 5). Crevasse

333   splay elements in the Morrison Formation have average width of 181 m (71 m to 360 m,

334   n=6), average length of 280 m (94 m to 540 m, n=9) and average thickness of 0.9 m (0.2 m to

335   2.1 m, n=45). Crevasse splay elements in the Castlegate Sandstone have average width of

336   353 m (300 m to 405 m, n=2), average length of 559 m (417 m to 700 m, n=2) and average

337   thickness of 1.1 m (1.6 m to 2.6 m, n=4). Crevasse splay elements in the Neslen Formation

338   have average width of 1072 m (464 m to 1503 m, n=9), average length of 538 m (292 m to

339   586 m, n=4) and average thickness of 1.4 m (0.5 m to 3.6 m, n=25).

340   There are limitations when defining an element using established recognition criteria:

341   bounding surfaces may become amalgamated to form composite surfaces rendering the

342   tracing of discrete bodies problematic; fines, including floodplain siltstones that can be

343   variably pedogenised, are used to identify underlying and overlying bounding surfaces but

344   demonstration of palaeoenvironmental significance requires careful examination of outcrop

345   of sufficient lateral continuity and extent for positive identification of a floodplain origin;

346   associations of facies within elements can be highly variable depending on proximity to the

347   feeder river channel (Burns *et al.* 2017); establishment of geometries requires outcrop of

348   sufficient quality, lateral extent and continuity. Establishing the three-dimensional

349   geometries of exhumed elements is also problematic, with outcrop of sufficient quality

350   (extent, continuity, 3D trend) needed to define the planform morphology of the deposit.

351   Surface expressions of modern splays (Fig. 6) demonstrate the complexity and variability of

352   the planform shapes of these elements. Common planform shapes of splays identified from

353   modern examples include lobate, elongate (in orientations perpendicular or oblique to the

354   trend of the main channel), and irregular (Fig. 6A) (Jorgensen & Fielding 1996). Planform

355   lengths of modern splays are taken as the greatest distance perpendicular to the main

356   channel, and widths are measured in orientations perpendicular to the lengths (Fig. 6). In

357   the studied modern examples, lobate splays are smooth-edged with widths averaging 683 m

358   (73 m to 2,252 m, n=65), and lengths averaging 703 m (51 to 2,650 m, n=65); elongate

359   splays are smooth-edged with longer lengths, averaging 1,155 m (324 to 3,574 m, n=31),

360   than widths, averaging 599 m (149 to 2,179 m, n=31), and tend to be elongate in the

361   direction of main river flow; splay bodies with irregular shapes have uneven edges and can

362   have the greatest range of width, averaging 723 m (179 to 2,087 m, n=25), and lengths,

363   averaging 731 m (301 to 1,847 m, n=25) (Fig. 7).

364   *Crevasse-channel fill (CR)*

365   Bounding surfaces that define the base of crevasse-channel fills are erosional, with relief

366   between 0.5 to 1.5 m. The top surfaces of crevasse-channel elements can be either sharp

367   (Fig. 4) if the crevasse-channel-fill is sandstone-prone throughout (Fig. 4) or gradational if

368   the crevasse-channel element is infilled with finer sediments.

369   The most common lithofacies associations in crevasse-channel fills differ between examples

370   in the Morrison Formation and in the Mesaverde Group. In the Mesaverde Group,

371   structureless sandstones (Sm) (53% Neslen Formation) planar cross-stratified sandstones

372 (Sp) (16% Castlegate Sandstone, 32% Neslen Formation) deformed sand facies (Sd) (16%

373 Neslen Formation) and deformed silt facies (58% Castlegate Sandstone) are the most

374 common facies (Fig. 5). By contrast, in the Morrison Formation structureless sandstones

375 (Sm) (95%) dominate. Stratigraphically, crevasse-channel fill elements show different types

376 of accumulations. Some crevasse channel-fills only comprise one or two types of facies

377 vertically (Fig. 4), whereas others consist of sand facies such as structureless sandstones and

378 planar cross-bedded sandstones overlain by deformed sandstones and siltstones and poorly

379 sorted siltstones. Ancient outcrop crevasse-channel fills are 6 to 30 m wide (average 20 m)

380 and 0.6 m to 5 m thick (2.85 m average, n=11), and may incise into other floodplain

381 elements (Fig. 5).

382 The expression of modern crevasse channel networks (Fig. 6B) demonstrates how crevasse

383 channels networks vary in development before they are ultimately infilled; some modern

384 crevasse channel networks are simpler in form than others (e.g. Fig. 6B), yet others develop

385 into more complicated bifurcating channel networks (e.g. Fig. 6A).

386 *Floodplain element (FF)*

387 Basal bounding surfaces in floodplain elements are flat-lying and non-erosional. Rooted

388 horizons can be found and are common in this element-type. Upper bounding surfaces with

389 overlying and underlying splay or channel-fill deposits are sharp (Fig. 4). Stratigraphic

390 transitions between two floodplain elements are gradational where intense bioturbation or

391 rooted horizons overprint the primary structures of the sediments. The floodplain elements

392 of the Castlegate and Neslen formations are coal-prone, and comprise laminated, organic-

393 rich siltstone (Fl) (76% Castlegate Sandstone, 88% Neslen Formation), less heavily rooted

394 siltstone (Fr) (24% Castlegate Sandstone) and coal (C) (12% Neslen Formation) (Fig. 5). By

395 contrast, floodplain elements of the Morrison Formation are heavily rooted (Table 1; Fig. 5),

396 with greater proportion of pedogenised facies (Frr 24% and Frg 6 %), as well as mottled

397 siltstones (Frm 28%) and laminated organic rich siltstones (Fl 42%). In the Morrison

398 Formation, different types of rooted siltstones can pass vertically in a gradational style from

399 one to another (Fig. 4). In the Mesaverde Group, examples of well-laminated siltstones,

400 sometimes with roots, are interbedded with coals (Fig. 4). These units form laterally

401 extensive sheets with thicknesses that are constant for tens of metres, maximum value

402 observed in this study 240 m (Fig. 5). Floodplain elements from the ancient outcrop have an

403 average minimum length of 69 m (22 to 240 m, n=30) and an average thickness of 0.73 m

404 (0.1 to 1.95 m, n=54). In the Morrison Formation, minimum lengths average 66 m (22 to 240

405 m, n=19) and thicknesses average 0.8 m (0.05 m to 2.9 m, 72). In the Castlegate Sandstone,

406 thicknesses average 0.7 m (0.2 to 2.2 m, n=23). In the Neslen Formation minimum lengths

407 average 78 m (50 m to 156 m, n=11) and thicknesses average 0.6 m (0.3 m to 1 m, n=42). In

408 the Castlegate and Neslen formations, floodplain elements are associated with coal-prone

409 floodplain elements, and the distal edges of splays are seen to pass gradationally into

410 floodplain deposits (Burns *et al.* 2017). The degree of pedogenesis varies in each of the

411 studied formations: the Morrison Formation exhibits the greatest degree of pedogenesis

412 comparable to the intense pedogenesis observed by other workers (Abels *et al.* 2013).

413 Pedogenesis in the Castlegate Sandstones is minimal or incipient, whereas pedogenesis in

414 the Neslen Formation is moderate (cf. Abels *et al.* 2013)

415

416 **Splay complexes**

417 *Defining a splay complex*

418 The uppermost level of the hierarchy is the splay complex and consists of the three

419 previously introduced overbank elements (Fig. 1). Complexes must comprise two or more

420 splay elements, as they do in the studied examples (Figs 8 & 9) – although this characteristic

421 is difficult to recognize in distal parts of the studied complexes (Fig. 8C). In the studied

422 successions, complexes also exhibit overall thinning and fining trends in the distal direction,

423 i.e., away from the channel body that represents the deposits of the formative river. In

424 proximal reaches complexes will tend to have indicators of similar palaeoflow direction

425 (average of the outcrop examples in this study have a standard deviation of 39.3 degrees in

426 each of the individual splay elements and 33.3 degrees in each of the individual complexes).

427 Splay complexes in the studied successions are generally thicker than the splay element it

428 contains, and are generally thicker than the average element thickness for that study

429 succession (Fig. 7A; Fig. 9). Splay complexes also originate from the same breakout point in

430 the levee (Fig. 11), and consequently can be traced (outcrop permitting) to the same parent

431 channel (Figs 8A & 9 CH1/C3). Splay complexes for all formations considered in this study

432 are over 3 m thick, whereas an element is typically under 3 m thick (Fig. 7A). In the Morrison

433 Formation, splay complexes are thinner, on average 3.4 m (1.3 m to 6.8 m, n=5), than those

434 recognised in the Neslen Formation, on average 6 m (2.7 m to 9.6 m, n=7) (Fig. 7A).

435 Elements within complexes can be vertically superposed, but each of the elements present

436 must be definable by identifiable, sharp bounding surfaces. Such relationships are especially

437 evident in proximal areas of a complex, whereas in more distal regions splay elements can

438 intercalate with floodplain elements by interdigitation (Fig. 8C).

439 A complex will be directly underlain and overlain by fine-grained deposits (Fig. 9); such

440 deposits represent a period of time where splay deposition was inactive at that point on the

441 floodplain. Consequently, deposits that encase complexes will represent non-crevasse-

442 related sedimentation, such as coals or laminated organic rich siltstones that contain roots,

443 and will likely record pedogenesis (Fig. 9).

444 Similar to splay elements, there is a consistent proximal to distal thinning and fining trend in

445 splay complexes, away from the channel-belt. The elements within a complex tend to show

446 comparable palaeoflow directions in the proximal and medial areas (Figs 8 & 10), and ranges

447 in palaeocurrent directions in complexes (060° to 240°) are comparable to those observed in

448 single elements (040° to 220°). Towards the distal end of the splay complex, palaeoflow

449 indicators are rare. Splay elements that are not genetically related although vertically

450 stacked may not show comparable palaeoflow directions (Fig. 8). The lateral extents of

451 complexes vary in the studied successions, with lengths between 130 m and 1,502 m,

452 averaging 835 m: in the Morrison Formation complex lengths average 242 m (130 m to 390

453 m), whereas in the Neslen Formation complex lengths average 1,169 m (160 m to 1,502 m)

454 (Fig. 7A).

455 Internally, a complex will show various stacking patterns and styles. Splay elements can

456 stack compensationally (Fig. 8A). Younger splay elements within a complex can also be

457 truncated erosionally, so that reduction in the thickness of older splays is particularly

458 common in the proximal areas where splay elements are eroded and amalgamated (Fig. 8A).

459 Complexes that show amalgamated sand-on-sand contacts between splay elements might

460 instead interfinger with floodplain elements in their medial or distal parts (Fig. 8C); in some

461 cases individual beds within splay elements occur interbedded with floodplain deposits

462 producing complicated splitting geometries (Fig. 8C).

463 In the studied ancient successions, splay complexes have been recognised to exhibit

464 compensational stacking styles, marked by lateral variations in the thickness of the deposits

465 (Fig. 11D); however, no progradational stacking trends were recognised in the studied units.

466 In modern systems, splay complexes have plan-view shapes similar to those of splay

467   elements. Individual active splay elements within the complex can be identified by distinct

468   crevasse-channel network; each individual splay element infills an area adjacent to the

469   previously active splay, in either a compensational style (Fig. 11B) or with a mixed

470   compensational and progradational style (Figs 11A–C).

471   At a larger scale, genetically unrelated splay complexes that emanated from breakout points

472   associated with different reaches of one or more parent rivers can overlap within the

473   floodbasin to build amalgamated successions (Fig. 1; Fig. 11G).

474

Discussion

Stacking patterns of splay elements

477   Stacking patterns of splay elements in splay complexes include compensational stacking,

478   which was recognised in the studied ancient successions (Fig. 11D; Donselaar *et al.* 2013; Li

479   *et al.* 2014; van Toorenenburg *et al.* 2016; Gulliford *et al.* 2017) and progradational stacking,

480   which was recognised in the modern examples and in other studies (cf. Buehler *et al*. 2011;

481   van Toorenenburg *et al.* 2016). Compensational stacking is a product of local

482   accommodation conditions (Brown 1979): splay deposition creates topographic highs on the

483   floodplain and subsequent splay deposits will occupy the adjacent topographic lows

484   (Donselaar *et al.* 2013; van Toorenenburg *et al.* 2016; Donselaar *et al.* 2017; Gulliford *et al*.

485   2017). Compensational stacking patterns are more likely to occur where the gradient of the

486   floodplain is such that the resultant slope drives floodwaters parallel to the major trunk

487   channel (cf. Wright & Marriott 1993). The higher width-to-length ratios of elements in the

488   studied intervals of the Castlegate and Neslen formations indicate that palaeoflow in splay

489   deposits of these systems was dominantly parallel to the direction of the associated channel

490   belt; this may be indicative of a situation in which compensational stacking is the dominant

491   stacking style. Compensational stacking was also documented in the Morrison Formation

492   (Fig. 11D).

493   By contrast, progradational stacking was not recognised in the studied successions, but was

494   seen in the studied modern examples (Fig. 11). Progradational stacking trends in splay

495   complexes would require strong erosive floodwaters and/or a confined floodbasin to funnel

496   the floodwaters and producing a more elongate plan-view shape. Progradational stacking

497 styles in splay accumulations would also require a floodplain substrate that consisted of

498 compactable material, which could produce an increase in local accommodation into which

499 the complex could then build (cf. Nadon 1998; Törnqvist *et al.* 2008). Compensational and

500 progradational stacking patterns in splay complexes are end-members. It is likely that many

501 splay complexes will display components of both styles (cf. van Toorenenburg *et al.* 2016).

502

503 **Recognition of splay-complexes in the rock record**

504 A complex can be easier to recognise in the proximal reaches where the stacked elements

505 are better defined and have similar palaeoflows. In distal locations, recognition of a complex

506 is more challenging as there are limited palaeocurrent indicators, and splay elements

507 intercalate and pass laterally into floodplain elements (Figs 8 & 12B). The intercalation of

508 distal splay elements and floodplain fines could be the expression of a splay complex, or a

509 stack of non-genetically related splay-elements being deposited into the same floodbasin

510 (Fig. 13B).

511 By definition, a splay complex comprises more than one element. However, in some

512 locations a complex will be represented by a single splay element, or will display

513 amalgamation of elements that can make identification of individual elements within the

514 complex difficult. An element that is part of a complex will not be overlain everywhere by

515 the subsequent element in the complex due to compensational stacking (Fig. 12A). In the

516 proximal areas, the complex can be preserved in the rock record as a thick stack of several

517 splay elements, as a stack of partially preserved elements (Fig. 13C). The presence of fine-

518 grained deposits that mark the occurrence of bounding surfaces is very important in the

519 identification of splay complexes (Gulliford *et al*. 2017). In this study, the deposits used to

520 recognize different scales of splay deposits are palaeosols and coals or laminated rooted

521 organic-rich floodplain siltstones (Fig. 5). Each one of these types of floodplain deposits

522 represents a period of time when splay deposition was not active on the floodplain at that

523 geographic location and can be used to delineate different scales of splay deposits.

524 Accumulated thickness is a useful guide but is not used as a criterion. For example, the

525 thickest splay element recorded in Neslen Formation is 3.7 m thick but the minimum

526 thickness of a recorded complex (with multiple definable splay elements within them and

527 bounded by fines) in the Morrison Formation is 1.3 m (Fig. 7A). Although, most complexes in

528 this study are greater than 3 m thick, aforementioned average thicknesses in the Morrison

529 Formation, at 3.4 m, are significantly lower than the average thicknesses from complexes

530 recognised in the Neslen Formation, at 6 m (Fig. 7A). The scaling differences are also true of

531 elements, with elements observed in the Morrison Formation having thicknesses

532 considerably lower than those in the Castlegate Sandstone and Neslen Formation (Fig. 7A).

533 The thinning and fining trends observed in both splay complexes and splay elements could

534 be used as an indicator of the position of major channel bodies, since these transitions scale

535 to the size of the river and the parent channel of the splay. In this study, parent channel

536 bodies were recorded as being an average of 4 m thick (1.6 m to 6.5 m, n=11), associated

537 splay element were recorded as having an average thickness of 0.9 m (0.2 m to 2.54 m

538 n=11); however, there are inherent uncertainties in these relationships because of the

539 difficult nature of ascribing a master channel to a particular splay element. Lateral

540 transitions between splay elements occurred within an average distance of ca. 500 m for the

541 studied ancient splay elements, and of ca. 1,000 m for the studied ancient splay complexes,

542 transitions occurred over ca. 670 m for the studied modern splays.

543 The differences between elements and complexes from the different formations could be

544 due to a number of reasons, such as scaling relationships with the parent channel, the scale

545 of the flood events resulting in splay accumulations, availability of sediment for deposition

546 of floodplain, accommodation space on the floodplain, and floodplain drainage conditions

547 (Pizzuto 1987; Williams 1989; Cazanacli & Smith 1998; Florsheim & Mount 2002; Adams *et*

548 *al.* 2004; Hajek & Wolinsky 2012; van Toorenenburg *et al.* 2016; Millard *et al.* 2017).

549 Two splay complexes can accumulate in the same floodbasin (e.g. Fig. 8C; Fig. 11G), which

550 will likely have different directions of palaeoflow and thinning and fining trends. If

551 deposition of the two complexes is non-contemporaneous and non-genetically related, it is

552 envisaged that the complexes would be stacked vertically and potentially separated by fine-

553 grained units (Fig. 8C), but such complexes would need to be traced out laterally to confirm

554 the stratigraphic relationships.

555 In modern systems, the relationships between different complexes are clearer where there

556 is lateral amalgamation of separate splay elements, which tends to occur at the lateral

557 fringes of the splay elements (Figs 11E–F), and of complexes, which might merge not only at

558 their lateral fringes but also at their distal ends (Fig. 11E). Lateral amalgamation of splay

559 elements can give rise to extensive sheets. Longitudinal and lateral merging of complexes

18

560 could result in overbank successions that predominantly comprise of splay deposits. In

561 general, genetically unrelated splay elements are likely to exhibit different thinning and

562 fining directions for individual elements, and substantial differences in palaeoflow directions

563 between elements (Fig. 10).

564 The identification of a splay complex must be undertaken with care; sufficient outcrop

565 exposure and fulfilment of the majority of the proposed recognition criteria are required.

566 Recognition of the manner in which splay complexes interact with one another, and how

567 this might be seen in a 1D dataset, have implications for predictions and conceptual models

568 of the subsurface (Fig. 10). However, many of the recognition criteria proposed, such as

569 lateral continuity and ability to trace laterally fine-grained units that mark their boundaries,

570 are not applicable to core data, and thickness observations can be misleading.

571

572 **Exportability of the hierarchy scheme**

573 In the chosen literature studies, facies and facies assemblages are utilized in a similar

574 manner to this study (Mjøs *et al.* 1993; van Toorenenburg *et al.* 2016; Gulliford *et al.* 2017).

575 Splay elements in the study of the Huesca fan succession (Ebro Basin, Spain) are defined

576 using architectural elements based on the facies assemblages (van Toorenenburg *et al.*

577 2016); these facies arrangements are similar to those in this study, but with a greater

578 prevalence of Sr and Sl facies; the nature of bounding surfaces is also comparable (i.e., sharp

579 lower boundaries). In the Huesca fan, splay elements are thinner (0.5- 0.6 m thick) (van

580 Toorenenburg *et al.* 2016) than those in this study.

581 Splay elements in the Beaufort Formation (Karoo Basin, South Africa) are also defined using

582 their bounding surfaces and internal facies arrangements (common facies as follows Sr, Sh,

583 Sm and Sl) and are comparable to the proximal-splay facies association recognised here

584 (Gulliford *et al.* 2017). Geometries of the splays in both this study and the Beaufort Group

585 are similar: tabular with lateral thinning and fining trends distally (Gulliford *et al.* 2017).

586 Crevasse-splay elements in the Beaufort Formation (0.5 m to 2 m) are larger than those in

587 the Huesca fan, (<2 m), and comparable to splay-elements in this study.

588 Crevasse-splay elements in the Ravenscar Group (Cleveland Basin, UK) are recognised using

589 facies assemblages (common facies include Sr, Sl, Sm, Sp; (cf. Fig. 7A), sharp basal

590 boundaries (occasionally gradational) and upper boundaries that are generally sharp but

591   sometimes gradational (Mjøs *et al.* 1993). The crevasse-splay elements of the Ravenscar

592   Group are similar in scale to the splay elements seen in the Neslen and Castlegate

593   formations, usually less than 1 m but up to 2.5 m in thickness.

594   The terminology used to describe these stacked deposits is different in each body of work.

595   Van Toorenenburg *et al.* (2016) use the term 'stacked splays' to describe stacked crevasse-

596   splay elements in the succession of the Huesca fan, and these are noted to be up to 2.4 m

597   thick. Gulliford *et al*. (2017) use the term 'splay stack' to describe stacked crevasse-splay

598   elements in the Beaufort Formation; these are noted as being up to 4 m thick and having a

599   lateral extent of around 700 m, which is comparable to the splay complexes in this study

600   (Figs 7 & 8). Mjøs *et al.* (1993) also recognised stacked and amalgamated splay deposits

601   using the term 'composite splay bodies', which are of very similar in thickness to the splay

602   complexes of this study (2.5 to 6 m), but with far greater lateral extent (up to 20 km) (Mjøs

603   *et al.* 1993).

604   Overall, the bounding surfaces, the internal facies arrangements and the relative geometries

605   of elements and complexes as documented in other studies are similar, but the terminology

606   used and the scales at which the deposits occur at are different. Since the components of

607   the hierarchy scheme proposed in this paper are recognisable in studies of overbank

608   deposits originating from markedly different systems, the terminology proposed in this

609   scheme appears well suited for comparisons of overbank deposits across depositional

610   systems. The splay elements recognised in the Huesca fan, Beaufort Formation and

611   Ravenscar Group study would also be classified in our hierarchy scheme as splay elements;

612   the stacked splays (Huesa Fan), splay stacks (Beaufort Formation) and composite splay

613   bodies (Ravenscar Group) would be classified in our hierarchy scheme as splay complexes.

614

615   **Conclusions**

616   A set of recognition criteria for defining splay elements and complexes is proposed, based

617   on bounding surfaces and adjacent deposits, facies arrangements including thinning and

618   finings trends, external geometries, and stratal patterns. The use of these criteria has

619   allowed a hierarchical scheme to be proposed, according to which splay deposits are

620   categorised into lithofacies, beds, elements and complexes in order to produce a unifying

621   scheme with which to better understand and compare such deposits. Both compensational

622   and progradational stacking are recognised as possible controls on the stratal architecture

623   of splay deposits. The relative dominance of each of the two types within a crevasse

624   complex will be a result of available floodplain accommodation and its spatial distribution in

625   relation to floodplain physiography. Splay deposits can amalgamate laterally to form wide

626   sand-prone bodies, representing either elements or complexes, and might stack vertically in

627   genetically related complexes. Lateral merging of splays is more likely to occur than merging

628   at their longitudinal margins. Vertical connectivity of sands depends on the stacking style of

629   the sand-prone proximal parts of deposits, whether this be at element-scale or complex-

630   scale.

631   Previous studies on crevasse-splay deposits in the Ravenscar Group, Huesca fan and

632   Beaufort Formation have been chosen to illustrate the exportability of the approach in

633   systems under different climatic regimes and environmental settings. Although the scales of

634   the deposits vary, each example still displays similarities with respect to bounding surfaces,

635   facies assemblages and geometries described in the scheme introduced here. This suggests

636   that the recognition criteria proposed herein might be widely applicable to many other

637   systems.

638

649

650 **References**

651 Abels, H.A., Kraus, M.J. & Gingerich, P.D. 2013. Precession-scale cyclicity in the fluvial lower
652 Eocene Willwood Formation of the Bighorn Basin, Wyoming (USA). *Sedimentology*, **60**,
653 1467–1483.

654 Adams, P.N., Slingerland, R.L. & Smith, N.D. 2004. Variations in natural levee morphology in
655 anastomosed channel flood plain complexes. *Geomorphology,* **61**, 127–142.

656 Allen, J. R. L. 1966. On bed forms and palaeocurrents. *Sedimentology,* **6**, 153–190.

657 Allen, J.R.L. 1983. Studies in fluviatile sedimentation: Bars, bar-complexes and sandstone
658 sheets (low-sinuosity braided streams) in the Brownstones (L. Devonian), Welsh borders.
659 *Sedimentary Geology,* **33**, 237–293.

660 Armstrong, R.L. 1968. Sevier orogenic belt in Nevada and Utah. *Geological Society of*
661 *America Bulletin*, **79**, 429–458.

662 Arnaud-Fassetta, G. 2013. Dyke breaching and crevasse-splay sedimentary sequences of the
663 Rhône Delta, France, caused by extreme river-flood of December 2003. *Geografia Fisica e*
664 *Dinamica Quaternaria,* **36**, 7–26.

665 Bown, T.M. & Kraus, M.J. 1987. Integration of channel and floodplain suites; I,
666 Developmental sequence and lateral relations of alluvial Paleosols. *Journal of Sedimentary*
667 *Research*, **57,** 587–601.

668 Bridge, J.S. 1984. Large-scale facies sequences in alluvial overbank environments*. Journal of*
669 *Sedimentary Research,* **54**, 85–170.

670 Bridge, J.S. 1993. Description and interpretation of fluvial deposits: a critical perspective.
671 *Sedimentology,* **40**, 801–810.

672 Bridge, J.S. 2006. Fluvial facies models: recent developments. *In*: Posamentier, H.W.,
673 Walker, R.G. (eds.) *Facies Models Revisited. SEPM Special Publication,* **84***,* 85–117.

674 Brierley, G.J., Ferguson, R.J. & Woolfe, K.J. 1997. What is a fluvial levee? *Sedimentary*
675 *Geology,* **114**, 1–9.

676 Brookfield, M., 1977. The origin of bounding surfaces in ancient aeolian sandstones.
677 *Sedimentology,* **24**, 303–332.

678   Brown, L. F. 1979. Deltaic sandstone facies of the Mid-Continent. *In*: N.J. Hyne (eds.)

679   *Pennsylvanian Sandstones of the Mid-Continent*. *Tulsa Geological Society*, **SP1**, 35–63.

680   Buehler, H.A., Weissmann, G.S. Scuderi, L.A. & Hartley, A.J. 2011. Spatial and temporal

681   evolution of an avulsion on the Taquari River distributive fluvial system from satellite image

682   analysis. *Journal of Sedimentary Research,* **81**, 630–640.

683   Burns C.E., Mountney N.P. Hodgson D.M. & Colombera L. 2017. Anatomy and dimensions of

684   fluvial crevasse-splay deposits: Examples from the Cretaceous Castlegate Sandstone and

685   Neslen Formation, Utah, U.S.A. *Sedimentary Geology*, **351**, 21–35.

686   Burton, D., Flaig, P.P. & Prather, T.J. 2016. Regional Controls On Depositional Trends In

687   Tidally Modified Deltas: Insights From Sequence Stratigraphic Correlation and Mapping of

688   the Loyd And Sego Sandstones, Uinta And Piceance Basins of Utah and Colorado, USA.

689   *Journal of Sedimentary Research*, **86**, 763–785.

690   Campbell, C.V. 1967. Lamina, laminaset, bed and bedset. *Sedimentology*, **8**, 7–26.

691   Cazanacli, D. & Smith, N.D. 1998. A study of morphology and texture of natural levees-

692   Cumberland Marshes, Saskatchewan, Canada. *Geomorphology*, **25**, 43–55.

693   Cole, R. 2008. Characterization of fluvial sand bodies in the Neslen and lower Farrer

694   formations (Upper Cretaceous), Lower Sego Canyon, Utah. In: Longman, M.W., Morgan, C.D.

695   (eds) *Hydrocarbons Systems and Production in the Uinta Basin, Utah. Rocky 14 Mountain*

696   *Association of Geologists—Utah Geological Association Publication,* **37**, 81–100.

697   Coleman, J.M. 1969. Brahmaputra river: Channel processes and sedimentation Brahmaputra

698   river: Channel processes and sedimentation. *Sedimentary Geology*, **3**, 129–239.

699   Colombera, L., Mountney, N.P. & McCaffrey, W.D. 2012. A relational database for the

700   digitization of fluvial architecture: concepts and example applications. *Petroleum*

701   *Geoscience*, **18**, 129-140.

702   Colombera, L., Mountney, N.P. & McCaffrey, W.D. 2013. A quantitative approach to fluvial

703   facies models: Methods and example results. *Sedimentology*, **60**, 1526–1558.

704   Currie, B.S. 1997. Sequence stratigraphy of nonmarine Jurassic–Cretaceous rocks, central

705   Cordilleran foreland-basin system. *Geological Society of America Bulletin*, **109**, 1206–1222.

706   Decelles, P.G. & Burden, E.T. 1991. Non-marine sedimentation in the overfilled part of the

707   Jurassic–Cretaceous Cordilleran foreland basin: Morrison and Cloverly formations, central

708   Wyoming, USA: *Basin Research*, **4**, 291–313.

709   Decelles, P.G. & Currie, B.S. 1996. Long-term sediment accumulation in the Middle Jurassic–

710   early Eocene Cordileran retroarc foreland-basin system. *Geology,* **24**, 591–594

711   Demko, T.M., Currie, B.S. & Nicoll, K.A. 2004. Regional paleoclimatic and stratigraphic

712   implications of paleosols and fluvial/overbank architecture in the Morrison Formation

713   (Upper Jurassic), Western Interior, USA. *Sedimentary Geology*, **167**, 115–135.

714   Donselaar, M.E., Cuevas Gozalo, M.C. & Moyano, S. 2013. Avulsion processes at the

715   terminus of low-gradient semi-arid fluvial systems: lessons from the Río Colorado Altiplano

716   endorheic basin, Bolivia. *Sedimentary Geology*, **283**, 1–14.

717   Donselaar, M.E., Gozalo, M.C. & Wallinga, J. 2017. Avulsion History of a Holocene Semi-arid

718   River System-Outcrop Analogue for Thin-bedded Fluvial Reservoirs in the Rotliegend Feather

719   Edge*. In*: 79th EAGE Conference and Exhibition 2017.

720   Ethridge, F.G., Skelly, R.L. & Bristow, C.S. 1999. Avulsion and Crevassing in the sandy,

721   braided Niobrara River: complex response to base-level rise and aggradation. *In*: Smith, N.

722   D. & Rogers, J. (eds) *Fluvial Sedimentology VI. Special Publication of the International*

723   *Association of Sedimentologists*, **28***,* 179–191.

724   Farrell, K.J. 1987. Sedimentology and facies architecture of overbank deposits of the

725   Mississippi River, False River region, Louisiana. *In*: Ethridge, F.G Flores, R.M. & Harvey, M.D.

726   (eds) *Recent Developments in Fluvial Sedimentology. Society Economic Palaeontology*

727   *Mineral Special Publications*, **39**, 111–121.

728   Farrell, K.M. 2001. Geomorphology, facies architecture, and high-resolution, non-marine

729   sequence stratigraphy in avulsion deposits, Cumberland Marshes, Saskatchewan.

730   *Sedimentary Geology*, **139**, 93–150.

731   Fedele, J.J. & Paola, C., 2007. Similarity solutions for fluvial sediment fining by selective

732   deposition. *Journal of Geophysical Research: Earth Surface*, **112**, F02038.

733   Fielding, C. R. 1984. Upper delta plain lacustrine and fluviolacustrine facies from the

734   Westphalian of the Durham coalfield, NE England. *Sedimentology*, **31**, 547–567.

735 Fisher, J.A., Krapf, C.B.E. Lang, S.C. Nichols, G.J. & Payenberg, T.H.D. 2008. Sedimentology

736 and architecture of the Douglas Creek terminal splay, Lake Eyre, central Australia.

737 *Sedimentology*, **55**, 1915–1930.

738 Florsheim, J.L., & Mount, J.F. 2002. Restoration of floodplain topography by sand-splay

739 complex formation in response to intentional levee breaches, Lower Cosumnes River,

740 California. *Geomorphology*, **44**, 67–94.

741 Ford, G.L. & Pyles, D.R. 2014. A hierarchical approach for evaluating fluvial systems:

742 Architectural analysis and sequential evolution of the high net-sand content, middle

743 Wasatch Formation, Uinta Basin, Utah. *AAPG Bulletin*, **98**, 1273–1304.

744 Franczyk, K.J., Pitman, J.K. & Nichols, D.J. 1990. Sedimentology, mineralogy, palynology, and

745 depositional history of some uppermost Cretaceous and lowermost Tertiary rocks along the

746 Utah Book and Roan Cliffs east of the Green River. *US Government Printing Office, USGS*

747 *Bulletin*, 1-27.

748 Fricke, H.C., Foreman, B.Z. & Sewall, J.O. 2010. Integrated climate model-oxygen isotope

749 evidence for a North American monsoon during the Late Cretaceous. *Earth and Planetary*

750 *Science Letters*, **289**, 11–21.

751 Friend, P.F. 1983. Towards the field classification of alluvial architecture or sequence. *In:*

752 Collinson, J.D. & Lewin, J. (eds*), Modern and ancient fluvial systems, Internat. Assoc.*

753 *Sedimentologists Special Publication,* **6**, 345–354.

754 Gates, T.A., & Scheetz, R. 2015. A new saurolophine hadrosaurid (Dinosauria: Ornithopoda)

755 from the Campanian of Utah, North America. *Journal of Systematic Palaeontology,* **13**, 711–

756 725.

757 Gulliford, A.R., Flint, S.S. & Hodgson, D.M. 2017. Crevasse splay processes and deposits in an

758 ancient distributive fluvial system: The lower Beaufort Group, South Africa. *Sedimentary*

759 *Geology,* **358**, 1–18.

760 Hackney, C., Darby, S. Parsons, D. Leyland, J. Aalto, R. Nicholas, A. & Best, J. 2015, April.

761 Crevasse-splay sedimentation processes revealed through high resolution modelling. *In EGU*

762 *General Assembly Conference Abstracts* **17**.

763 Hajek, E.A. & Wolinsky, M.A. 2012. Simplified process modeling of river avulsion and alluvial

764 architecture: connecting models and field data. *Sedimentary Geology,* **257**, 1–30.

765   Hasiotis, S. T., 2004. Reconnaissance of Upper Jurassic Morrison Formation ichnofossils,

766   Rocky Mountain Region, USA: paleoenvironmental, stratigraphic, and paleoclimatic

767   significance of terrestrial and freshwater ichnocoenoses. Sedimentary Geology 167, 177-

768   268.

769   Hartley, A. J., Owen, A. Swan, A. Weissmann, G. S. Holzweber, B. I.,Howell, J. Nichols, G. &

770   Scuderi, L. 2015. Recognition and importance of amalgamated sandy meander belts in the

771   continental rock record. *Geology,* **43**, 679–682.

772   Hettinger, R.D., & Kirschbaum, M.A. 2002. Stratigraphy of the Upper Cretaceous Mancos

773   Shale (upper part) and Mesaverde Group in the southern part of the Uinta and Piceance

774   basins, Utah and Colorado. *US Geological Survey*, Pamphlet to accompany geologic

775   investigations series i–2764.

776   Holbrook, J. 2001. Origin, genetic interrelationships, and stratigraphy over the continuum of

777   fluvial channel-form bounding surfaces: an illustration from middle Cretaceous strata,

778   southeastern Colorado. *Sedimentary Geology*, **144**, 179–222.

779   Huber, B.T., Norris, R.D. & MacLeod, K.G. 2002. Deep-sea paleotemperature record of

780   extreme warmth during the Cretaceous. *Geology,* **30**, 123–126.

781   Jordan, D.W., & Pryor, W.A. 1992. Hierarchical levels of heterogeneity in a Mississippi River

782   meander belt and application to reservoir systems. *AAPG Bulletin*, **76**, 1601–1624.

783   Jorgensen, P. J. & Fielding, C. R. 1996. Facies architecture of alluvial floodbasin deposits:

784   three-dimensional data from the Upper Triassic Callide Coal Measures of east-central

785   Queensland, Australia. *Sedimentology*, **43**, 479–495.

786   Karaman, O. 2012. Shoreline Architecture and Sequence Stratigraphy of Campanian Iles

787   Clastic Wedge, Piceance Basin, CO: Influence of Laramide Movements in Western Interior

788   Seaway. University of Texas at Austin, Texas, p. 137.

789   Kauffman, E.G. 1977. Geological and biological overview: Western Interior Cretaceous

790   basin. *The Mountain Geologist*, **6**, 227–245.

791   Kraus, M.J. 1987. Integration of channel and floodplain suites; II, Vertical relations of alluvial

792   Paleosols. *Journal of Sedimentary Research*, **57,** 602–612.

793 Kraus, M.J. 1999. Paleosols in clastic sedimentary rocks: their geologic applications. *Earth-*
794 *Science Reviews*, **47**, 41–70.

795 Kirschbaum, M.A. & Hettinger, R.D. 2004. *Facies analysis and sequence stratigraphic*
796 *framework of Upper Campanian Strata (Neslen and Mount Garfield Formations, Bluecastle*
797 *Tongue of the Castlegate Sandstone, and Mancos Shale), Eastern Book Cliffs, Colorado and*
798 *Utah.* United States Geological Survey Digital Data Report **DDS-69-G**.

799 Kocurek, G. 1981. Significance of interdune deposits and bounding surfaces in aeolian dune
800 sands. *Sedimentology,* **28**, 753–780.

801 Lawton, T.F. 1994. Tectonic setting of Mesozoic sedimentary basins, Rocky Mountain region,
802 United States. *In:* Caputo, M.V., Peterson, J.A., & Franczyk, K.J. (eds) *Mesozoic Systems of*
803 *the Rocky Mountain Region, USA*. SEPM, Rocky Mountain Section 1–25.

804 Li, J., Donselaar, M.E. Hosseini Aria, S.E. Koenders, R. & Oyen, A.M. 2014. Landsat imagery
805 based visualization of the geomorphological development at the terminus of a dryland river
806 system. *Quaternary International*, **352**, 100–110.

807 Miall, A.D. 1985. Architectural-element analysis: a new method of facies analysis applied to
808 fluvial deposits. *Earth-Science Reviews*, **22**, 261–308.

809 Miall, A.D. 1988. Facies architecture in clastic sedimentary basins. *In*: Kleinspehn, K.L. &
810 Paola, C. (eds) *New Perspectives in Basin Analysis*. Springer-Verlag, New York 67–81.

811 Miall, A.D. 1993. The architecture of fluvial-deltaic sequences in the upper Mesaverde
812 Group (Upper Cretaceous), Book Cliffs, Utah. *In*: Best, J.L. Bristow, C. (eds) *Braided Rivers.*
813 *Geological Society of London, Special Publications,* **75**, 305–332.

814 Miall, A.D. 2014. *Fluvial Depositional Systems*, Springer. Berlin.

815 Middelkoop, H. & Asselman, N.E. 1998. Spatial variability of floodplain sedimentation at the
816 event scale in the Rhine–Meuse delta, The Netherlands. *Earth Surface Processes and*
817 *Landforms*, **23***,* 561–573.

818 Millard, C., Hajek, E. & Edmonds, D.A., 2017. Evaluating Controls On Crevasse-Splay Size:
819 Implications For Floodplain-Basin Filling. *Journal of Sedimentary Research*, **87**, 722–739.

820   Miller, I.M., Johnson, K.R. & Kline, D.E. 2013. A Late Campanian flora from the Kaiparowits.

821   *In*: Titus, A.L., Loewen, M.A. (eds.). *At the Top of the Grand Staircase: The Late Cretaceous of*

822   *Southern Utah.* Indiana University Press, Bloomington 107–131.

823   Mjøs, R., Walderhaug, O. & Prestholm, E., 1993. Crevasse splay sandstone geometries in the

824   Middle Jurassic Ravenscar Group of Yorkshire, UK. *In:* Marzo, M., & Puigdefabregas, C. (eds)

825   Alluvial Sedimentation. *International Association of Sedimentologists, Special Publication,* **17**,

826   167–184.

827   Morozova, G.S. & Smith, N.D., 2000. Holocene avulsion styles and sedimentation patterns of

828   the Saskatchewan River, Cumberland Marshes, Canada. *Sedimentary Geology*, **130**, 81–105.

829   Nadon, G.C. 1998. Magnitude and timing of peat-to-coal compaction. *Geology*, **26**, 727–730.

830   Nanson, G. & Croke, J. 1992. A genetic classification of floodplains. *Geomorphology*, **4**, 459–

831   486.

832   O'Brien, P. & Wells, A. 1986. A small, alluvial crevasse splay. *Journal of Sedimentary Petrology,*

833   **56**, 876–879.

834   O'Brien, K.C. 2015. Stratigraphic architecture of a shallow-water delta deposited in a coastal-

835   plain setting: Neslen Formation, Floy Canyon, Utah. Colorado School of Mines, Arthur Lakes

836   Library, p. 77.

837   Olsen, T., Steel, R. Hogseth, K. Skar, T. & Roe, S.L. 1995. Sequential architecture in a fluvial

838   succession: sequence stratigraphy in the Upper Cretaceous Mesaverde Group, Price Canyon,

839   Utah. *Journal of Sedimentary Research*, **65B**, 265–280.

840   Owen, A., Nichols, G.J. Hartley, A.J. Weissmann, G. S. & Scuderi, L. A. 2015. Quantification of

841   a Distributive Fluvial System: The Salt Wash DFS of the Morrison Formation, SW USA.

842   *Journal of Sedimentary Research,* **85**, 544–561.

843   Parker, G. 1991. Selective sorting and abrasion of river gravel. II: Applications. *Journal of*

844   *Hydraulic Engineering*, **117**, 150–171.

845   Pitman, J.K., Franczyk, K.J. & Anders, D.E. 1987. Marine and Nonmarine gas-bearing rocks in

846   Upper Cretaceous Neslen and Blackhawk formations, Eastern Uinta Basin, Utah-

847   Sedimentology, Diagenesis, and Source rock potential. *AAPG Bulletin*, **70**, 1052–1052.

848   Pizzuto, J.E. 1987. Sediment diffusion during overbank flows. *Sedimentology*, **34**, 301–317.

849   Prélat, A., Hodgson, D. & Flint, S. 2009. Evolution, architecture and hierarchy of distributary

850   deep-water deposits: a high-resolution outcrop investigation from the Permian Karoo Basin,

851   South Africa. *Sedimentology*, **56**, 2132–2154.

852   Robinson, J. W., & McCabe, P. J. 1998. Evolution of a braided river system: The Salt Wash

853   Member of the Morrison Formation (Jurassic) in southern Utah. *In*: Shanley, K. W., &

854   McCabe, P. J. (eds*). Relative Role of Eustasy, Climate, and Tectonism in Continental Rocks.*

855   Society of Sedimentary Geology, Special Publications, **59**, 93–107.

856   Seymour, D.L., & Fielding, C.R. 2013. High resolution correlation of the Upper Cretaceous

857   stratigraphy between the Book Cliffs and the western Henry Mountains Syncline, Utah,

858   USA. *Journal of Sedimentary Research*, **83**, 475–494.

859   Shanley, K.W., Mccabe, P.J. & Hettinger, R.D. 1992. Tidal influence in Cretaceous fluvial

860   strata from Utah, USA: a key to sequence stratigraphic interpretation. *Sedimentology,* **39**,

861   905–930.

862   Shen, Z., Törnqvist, T.E. Mauz, B. Chamberlain, E.L. Nijhuis, A.G. & Sandoval, L. 2015.

863   Episodic overbank deposition as a dominant mechanism of floodplain and delta-plain

864   aggradation. *Geology,* **43**, 875–878.

865   Shiers, M.S., Mountney, N.P. Hodgson, D.M. & Cobain, S.L. 2014. Depositional controls on

866   tidally influenced fluvial successions, Neslen Formation, Utah, USA. *Sedimentary Geology*,

867   **311**, 1–16.

868   Shiers, M.S., Hodgson, D.M. & Mountney, N.P., 2017. Response of a coal-bearing coastal

869   plain succession to marine transgression: Campanian Neslen Formation, Utah, U.S.A. *Journal*

870   *of Sedimentary Research,* **87**, 168–187.

871   Slingerland, R. & Smith, N.D., 1998. Necessary conditions for a meandering-river avulsion.

872   *Geology*, **26**, 435–438.

873   Slingerland, R., & Smith, N.D. 2004. River avulsions and their deposits. *Annual Review Earth*

874   *Planetary Science*, **32**, 257–285.

875   Smith, N.D., Cross, T.A. Dufficy, J.P. & Clough, S. R. 1989. Anatomy of an avulsion.

876   *Sedimentology*, **36**, 1–23.

877   Smith, N.D. & Perez-Arlucea, M. 1994. Fine-grained splay deposition in the avulsion belt of

878   the lower Saskatchewan River, Canada. *Journal of Sedimentary Research*, **64**, 159–168.

879   Sprague, A.R., Sullivan, M.D. Campion, K.M. Jensen, G.N. Goulding, F.J. Garfield, T.R.

880   Sickafoose, D.K. Rossen, C. Jennette, D.C. Beaubouef, R.T. Abreu, V. Ardill, J. Porter, M.L. &

881   Zelt, F.B. 2002. The physical stratigraphy of deep-water strata: a hierarchical approach to

882   the analysis of genetically related stratigraphic elements for improved reservoir prediction.

883   (Abstract) AAPG Annual Meeting. *AAPG Bulletin*, **87**, 1.

884   Taylor, A.M. & Goldring, R. 1993. Description and analysis of bioturbation and ichnofabric.

885   *Journal of the Geological Society*, ***150***, 141–148.

886   Toonen, W.H., Asselen, S. Stouthamer, E. & Smith, N.D. 2015. Depositional development of

887   the Muskeg Lake crevasse splay in the Cumberland Marshes (Canada). *Earth Surface*

888   *Processes and Landforms*, **37**, 459–472.

889   Törnqvist, T.E., & Bridge, J.S. 2002. Spatial variation of overbank aggradation rate and its

890   influence on avulsion frequency. *Sedimentology*, **49**, 891–905.

891   Törnqvist, T.E., Wallace, D.J. Storms, J.E. Walling, J. Van Dam, R.L. Blaauw, M. Derksen, M.S.

892   Klerks, C.J. Meijneken, C. & Snijders, E.M. 2008. Mississippi Delta subsidence primarily

893   caused by compaction of Holocene strata. *Nature Geoscience*, **1**, 173–176.

894   Van Toorenenburg, K.A., Donselaar, M.E. Noordijk, N.A. & Weltje, G.J., 2016. On the origin

895   of crevasse-splay amalgamation in the Huesca fluvial fan (Ebro Basin, Spain): Implications for

896   connectivity in low net-to-gross fluvial deposits. *Sedimentary Geology*, **343**, 156–164.

897   Van Wagoner, J.C., Mitchum, R.M. Campion, K.M. & Rahmanian, V.D. 1990. Siliciclastic

898   sequence stratigraphy in well logs, cores, and outcrops: concepts for high-resolution

899   correlation of time and facies. *AAPG Methods in Exploration Series.* AAPG Tulsa, Oklahoma,

900   55 pp.

901   Walker, R.G., & James, N. 1992. Facies, facies model and modern stratigraphic concepts.

902   Facies model: response to sea level change. *Geological Association of Canada*, 1–14.

903   Williams, G.P. 1989. Sediment concentration versus water discharge during single hydrologic

904   events in rivers. *Journal of Hydrology*, **111***,* 89–106.

905 Willis, A. 2000. Tectonic control of nested sequence architecture in the Sego Sandstone,

906 Neslen Formation and upper Castlegate Sandstone (Upper Cretaceous), Sevier foreland

907 basin, Utah, USA. *Sedimentary Geology*, 136, 277-317.

908 Wright, V.P. & Marriott, S.B. 1993. The sequence stratigraphy of fluvial depositional

909 systems: the role of floodplain sediment storage. *Sedimentary Geology*, **86**, 203–210.

910 **Figure captions**

911 **Fig. 1**. Overview of proposed hierarchical scheme for overbank deposits and splay deposits

912 in this paper. The lowest tier of the hierarchy are the facies and facies associations which

913 build into beds; the higher tier of the hierarchy comprises elements which can be single

914 beds with simple facies associations or can be multiple bed associations with several facies

915 types present; the highest tier of the hierarchy is the complex which is built of multiple splay

916 elements stacked together; splay complexes and element then comprise fluvial overbank

917 successions with amalgamated splay deposits.

918 **Fig. 2**. Stratigraphic columns introducing the studied formations and location map of field

919 sites. (**a**) The units treated in this study are the Saltwash Member of the Jurassic Morrison

920 Formation, the Campanian Castlegate Sandstone and the Campanian Neslen Formation;

921 after Robinson and McCabe (1998) and Kirschbaum and Hettinger (2004). (**b**) Map of the

922 study area. Yellow stars mark the position of the five Morrison field sites across Eastern

923 Utah and Western Colorado. Orange stars mark the position of the Castlegate Sandstone,

924 green stars mark the Neslen Formation field sites throughout the Book Cliffs in Eastern

925 Utah. (**c**) Illustration of the basin in which each of the formations accumulated adapted after

926 Armstrong (1968) Kauffman (1977), Seymour and Fielding (2013).

927

928 **Fig. 3**. Overview of complexity observed in studied splay elements (**a**) Examples of the

929 architectural-element types observed in the studied formations. (**b**) Splay element in the

930 Morrison Formation, which exhibits thinning and fining trend, away from the channel body

931 in log 1 towards the more distal end in log 2. (**c**) Crevasse-splay element made up of multiple

932 facies types vertically from the Neslen Formation, which transitions laterally from a cross-

933 bedded thicker sandstone body in log 3 to a finer grained succession on logs 2 and 1.

934

935   **Fig. 4**. Conceptual images of each element type recognised in this this study. Representative

936   logs and images of each of these overbank elements from the three studied formations:

937   Morrison Formation, Castlegate Sandstone and Neslen Formation. Sketch diagrams to

938   illustrate how the lengths and widths are defined in each of these element types.

939

940   **Fig. 5**. (**a**) Cross-plot graphs of element thickness plotted against element widths

941   (apparent)and lengths (apparent) for each of the three studied formations. (**b**) Plots of the

942   variations in thickness of each element type for each of the three studied formations. (**c**) Pie

943   charts demonstrating the proportions of each facies type that make-up each element type

944   for each of the studied formations.

945

946   **Fig. 6.** Examples of modern overbank elements. (**a**) CS: Crevasse-splay example from

947   Madagascar. These examples show the three types of crevasse-splay planform geometry

948   types: lobate, elongate and irregular. (**b**) CR: Crevasse-channel from the Paraná River, South

949   America. (**c**) AC: Abandoned channel and FF: Floodplain areas inferred to be dominated by

950   accumulation of fines, from the Paraguay River, South America (**d**) CF: floodplain area

951   inferred to be dominated by accumulation of organics, from the Paraguay River, South

952   America.

953

954   **Fig. 7**. Splay body dimensions from ancient and modern datasets (**a**): Lengths and widths of

955   ancient splay elements and complexes, plotted against thickness. Elements and complexes

956   measured in the Morrison Formation tend to have the lowest recorded widths, lengths and

957   thicknesses, whereas elements and complexes in the Neslen Formation have some of the

958   largest widths and thicknesses, with lengths only a little higher than those in the Morrison

959   Formation. Values from the Castlegate Sandstone tend to plot between the Morrison and

960   the Neslen formations for both length and widths (**b**): Widths and lengths of modern splays

961   from the Helodrano, Paraná, Saskatchewan, Saloum, Mississippi and East Madagascan

962   (Ankofia) rivers are plotted. Lobate splays show similar width to length ratios, elongate

963   splays show greater lengths than widths, and irregular splays show more variable ratios.

964

965   **Fig. 8**. Crevasse complexes from proximal to distal regions. (**a**) Example of proximal

966   crevasse-complex, coarsening upwards trend and thickening upwards trend. Logged

967 example and images are from the upper part of Neslen Formation at Crescent Canyon. (**b**)

968 Medial part of splay-complex, thickening and thinning of splay elements. Logged example

969 and photographs are from the Morrison Formation, medial portion of the Morrison fluvial

970 fan at Yellow Cat Canyon. (**c**): Distal part of crevasse-complex. Splays interbed with

971 floodplain fines. Logged example and photographs are from the lower part of the Neslen

972 Formation at Tuscher Canyon.

973

974 **Fig. 9**. (**a**) Photomontage of overbank succession from the Morrison Formation, Atkinson

975 Creek. Photomontage was taken from N 38°24'20.50 W 108°43'.00. (b) Interpreted

976 photomontage showing four splay complexes C1, C2, C3, the associated intervening fines

977 B1, B2, and B3, and channel deposits associated with C3. Splay deposits above B3 have not

978 been defined as a complex because of lack of palaeocurrents or clear relationship with a

979 channel body. Logged sections have been placed onto the photomontage grid co-ordinat4es

980 were taken for each: Log 1 N 38'39.901 W 108'74.673, Log 2 N 38'39.902 W 108'74.638, Log

981 3 N 38'39.941 W 108'74.628.

982

983 **Fig. 10**. Outcrop example from the upper part of the Neslen Formation; splay elements with

984 different thinning and fining directions, different palaeocurrent directions and interbedded

985 with floodplain fines, which are therefore interpreted as genetically unrelated splay

986 elements.

987

988 **Fig. 11**. Representative sattelite imargery and logged sections illustrating different stacking

989 styles in splay complexes (**a**) Genetically related splays from same breakout point,

990 Mississippi River. West (1) splay and North (2) splay no longer have active crevasse-

991 channels, while the Southern splay (3) has an active crevasse network. Each new splay is

992 building onto a different area on the floodplain in a compensational trend, however also,

993 the active splay is further onto floodplain than inactive ones which indicates some

994 progradational tendencies. (**b**) Genetically related splays from same breakout point, Paraná

995 River, South America. West (1) and South (2) crevasse-channel infilled, East (3) crevasse-

996 channel is still active. Each active splay builds laterally on the floodplain, compensational

997 trend (**c**) Genetically related splays, Saskatchewan River, Canada. Active crevasse-channels

998 in North (3) and West (4) splays whereas Southern splays (1 and 2) are inactive. Each new

999 splay is building onto a different area on the floodplain in a compensational trend, however

1000 also, the recent western splay (4) has built out further on to floodplain, a progradational

1001 trend. (**d**) Logged section from the Morrison Formation showing compensational stacking of

1002 splay elements and conceptual image to better illustrate the stacking (**e**) Genetically

1003 unrelated splays originating from different breakout points merging laterally, Volga River,

1004 Russia. Splays from different breakout points are merging laterally. (**f**) Genetically unrelated

1005 splay originating from different breakout points merging laterally Paraná River, South

1006 America. Splays from different breakouts merge laterally, the largest well-developed splay

1007 laterally amalgamates with the smaller splays. (**g**) Genetically unrelated splays originating

1008 from different breakout points merging longitudinally, Paraná River, South America. Two

1009 complexes laterally amalgamated coming from two separate breakout points in different

1010 flow directions.

1011

1012 **Fig. 12**. Overview of impact stacking styles and planform morphology on resultant

1013 stratigraphic architecture(**a**) Stacking patterns of splay elements in complex are variable;

1014 two-end member models are presented for stacking pattern styles: progradational stacking

1015 patterns and compensational stacking patterns. Progradational stacking patterns result in

1016 coarsening and thickening upwards and an elongate planform shape whereby the complex

1017 width is shorter than the length. Compensational stacking patterns result in different

1018 vertical profiles depending on planform position of the vertical section. These profiles range

1019 from: (i) no trend in vertical profile; (ii) fining and thinning-up trends; (iii) coarsening and

1020 thickening-upwards trends. This can result in the complex being represented by stacks of

1021 splays in some sections whereas elsewhere it might be represented only by a single

1022 element. (**b**): Stacking patterns in crevasse complexes and implications for sand

1023 connectivity. (**c**): Crevasse splay deposits can connect at the longitudinal fringes of the

1024 complexes or at their lateral margins. The latter scenario is more likely to produce larger

1025 bodies of preserved sand.

1026

1027 **Fig. 13**. Complications in splay complex identification: (**a**) Cartoon of temporal evolution of a

1028 system that illustrates different types of deposition of fines; as the main channel migrates

1029 away from a site of overbank deposition and crevassing ceases, floodplain fines will start to

1030 accumulate. Through time, palaeosols will start to develop. Rooting will indicate cessation of

1031 splay deposition. (**b**) Stacks of splay elements can accumulate in the same floodbasin either

1032 as genetically related complexes (i) or as non-related elements (ii). These situations result in

1033 architectures that appear very different in the proximal reaches but may be

1034 indistinguishable in the distal reaches. (**c**) A complex can be represented by a stack of splay

1035 elements or by a single splay element.

1036 **Table 1**. *Facies types documented in Morrison Formation and Mesaverde Group*

Code	Facies	Description	Interpretation
Gm	Green structureless conglomerate	Green, subangular pebble to conglomerate, poor to moderate sorting with very-fine to fine sandstone matrix. Sets 0.8- 2.4 m (1.7 m average). Sets are structureless, or show weak fining-upwards trend.	Bedload deposition from a relatively high-energy flow.
Gp	Cross-stratified conglomerate	Green-grey, subangular pebble to conglomerate, poor to moderately sorted in a very-fine to fine sandstone matrix. Individual sets 1.0- 2.3 m (1.5 m average). Cross-bedding common (0.8- 2.4 m)	Deposition from a relatively high-energy flow and downstream migration of gravelly bedforms.
St/Sp	Trough and planar cross-bedded sandstone	Grey-yellow-brown very fine to medium-grained sandstone, moderately well-sorted. Subangular to subrounded grains. Sets are 3- 12 m (4.6 m average) thick. Mud rip-up clasts and plant fragments are common. Trough and planar cross stratification common throughout sets 0.4- 1.5 m (1.0 m average).	Deposition from a relatively high-energy flow and downstream migration of sandy bedforms.
Sm	Structureless sandstone	Dark grey-yellow-brown, very-fine to fine sandstone, moderately to poorly sorted. Thickness ranges 0.2- 2.2 m (1 m	Records rapid deposition of sand

		average). Internally sets are structureless.	from suspension in a decelerating flow.
Sr	Small-scale ripple cross-laminated sandstone	Grey-yellow-brown, very-fine to fine sandstone, moderately to poorly sorted. Sets varying from 0.1- 4.1 m (1 m average). Small-scale ripple cross-laminations (0.1- 0.9 m) are common to this facies. Contains small (<50 mm long) plant fragments, bark pieces and coal fragments.	Down flow migration of ripple bedforms under an aggradational regime.
Sd	Soft-sediment deformed sandstone with remnant ripple forms	Grey-yellow-brown, very-fine to fine sandstone, poorly to moderately sorted. Sets vary from 0.4- 2.4 m (1.1 m average). Convolute lamination within sets and remnant ripples.	Records deposition from a mixed flow onto an unstable waterlogged substrate.
Fd	Soft-sediment deformed mixed sandstone and siltstones	Dark grey-yellow-brown, fine siltstone to very-fine sandstone, poorly sorted. Thicknesses vary from 0.1- 3 m (0.6 m average). Primary sedimentary structures are overprinted by soft-sediment deformation.	Records deposition from a mixed flow onto an unstable waterlogged substrate
Fp	Structureless poorly sorted rooted siltstones	Light-blue-grey, fine siltstone to very-fine sandstone, poorly sorted, Set thicknesses varies from 0.1- 2.1 m (0.6 m average). Sets of this facies are mostly structureless though some show weak fining-up trends. In situ and some carbonised anthracite material.	Poorly sorted and structureless silt-prone facies was deposited rapidly from suspended load.

Fop	Structureless organic-rich poorly sorted rooted siltstone	Dark grey, fine siltstone to very-fine sandstone, poorly sorted. Set thicknesses vary from 0.3- 2.1 m (0.8 m average). Sets are structureless with weak fining trend. Dispersed organic content and roots.	Deposited rapidly from suspended load.
Fm	Well sorted blue clean siltstones	Light blue, middle to coarse siltstone, well to moderately well sorted, rare occurrences of roots or plant material. Bases are erosional between 1-2 m. Set thicknesses vary from 0.4- 2.4 m (1.4 m average). Structureless or weakly laminated.	Siltstone represent deposition from low-energy suspension after an erosive event.
Fl	Laminated organic-rich siltstones	Medium to dark-grey, red, green siltstone, well to moderately well sorted. Thicknesses vary from 0.3- 1.1 m (0.7 m average) and grain size remains consistent throughout a bed. Planar lamination is common. Small plant roots (<10 mm) occur in the Morrison and wisps of anthracite in the Neslen.	Steady deposition from a low-energy flow.
C	Coal	Dark-grey to black, claystone, well-sorted. Sets vary from 0.2- 2.1 m (0.7 m average). Plant fragments and higher quality anthracite coal fragments present.	Records slow deposition, in organic-rich setting with limited clastic input.
Fr	Laminated rooted siltstones	Blue-grey to light grey, upper to lower siltstone, moderately well-sorted. Thicknesses vary from 0.2- 0.9 m (0.4 m average). Can be weakly laminated. Rooting common.	Well drained, gradual deposition under low-energy regime.

Frg	Green rooted siltstones	Green-grey, fine siltstone, well to moderately well-sorted. Thicknesses vary from 0.1- 2.7 m (0.6 m average). Can be weakly laminated. Plant root structures common (<5 mm width and length) but tend to be concentrated towards the top of sets.	Poorly drained, high water table, gradual deposition under low-energy regime.
Frr	Red rooted siltstones	Red, fine to coarse siltstone, Well to moderately well-sorted. Thicknesses vary from 0.1- 2.7 m (0.6 m average). Weakly laminated. Plant root structures common: sideritized, long (up to 10 cm) and thin (<5 mm) and taper towards base. Low to moderate intensity bioturbation and slickenlines present.	Well-drained, dry, calcisol, gradual deposition under low-energy regime.
Frm	Purple mottled rooted siltstones	Purple-red, fine to coarse siltstone, well to moderately well-sorted. Thicknesses vary from 0.3- 3.6 m (1.8 m average). Structureless. Small roots throughout (<5 mm), moderate to high intensity bioturbation. Mottled pale purple colour due to watermarks.	Poorly drained, higher water table, gradual deposition.

1037

① Facies

② Beds

5m

FA
multiple facies

FA
single facies

FA
multiple facies

0m

③ Splay-element

Single bed

| Proximal | Medial | Distal |

Multiple beds

④ Splay-complex

T1

T3 T2 T4

T5

T3

T2

T1
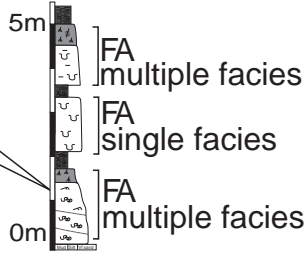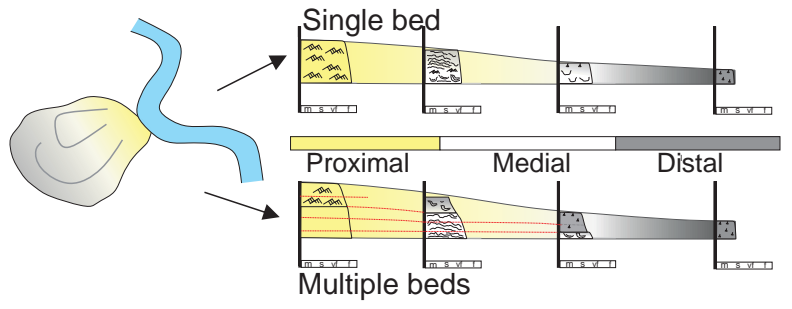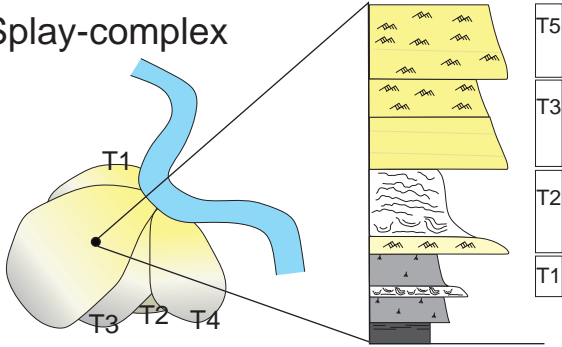
⑤ Fluvial overbank succession comprising amalgamated splay complexes derived from separate river break-out points

A

Ma				
152.1	Tithonian	Jurrassic	Morrison Formation	Brushy Basin Member
157.3	Kimmeridgian			Saltwash Member
163.5	Oxfordian			Tidwell Member
	Callovian			Summerville Formation
Ma				Entrada Sandstone

Ma		
75	Campanian	Neslen Formation
		Sego Sandstone
80		Buck Tongue of Mancos Shale
		Castlegate Sandstone
Ma		Blackhawk Formation

B

McInnis Canyon National
Fruita
Grand Junction
Cisco
Crescent Junction
Arches National Park
Moab
Gateway
Dominguez-Escalante National Conservation Area
Paradox
Uravan
La Sal
Naturita
Slick Rock
39°
38°
109°
N
0   30km

C

W — Proximal   E — Distal

overthrust Paleozoic strata
North Holm
Fox Hills Sst.
Price River Fm.
Mesaverde Group
Pierre Shale
Indianola Group
South Flat Fm.
Castlegate Sst.
80 Ma
Star Point Sst.
Blackhawk Fm.
Nodrara Limestone
Jurassic and Triassic strata
Funk Valley Fm.
Mancos Shale
Dakota Sst.
500 m
100 km
Morrison Fm. 152 Ma

A. Element types observed in Mesaverde Group and Morrison Formation
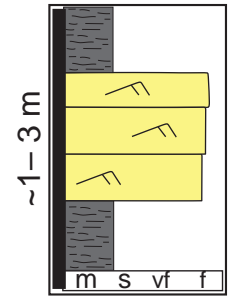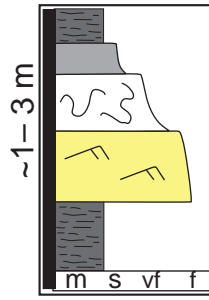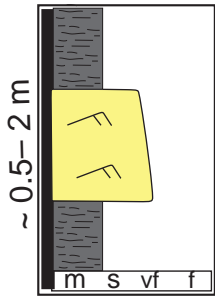
	~0.5–2 m	~1–3 m	~1–3 m
Neslen (n=104)	59.6%	37.5%	2.9%
Castlegate (n=48)	70.8%	10.4%	18.8%
Morrison (n=126)	70.6%	27.8%	1.6%

B. Single facies

C. Multiple facies

Crevasse-channel element

Fp
Fd
Sr

0m — 5m

Floy Canyon, Castlegate Sandstone

1 m
1 m
0 m

L
W

Crevasse-splay element

Fp
Fd
Sr
Sr

0m — 100m

Floy Canyon, Castlegate Sandstone

5 m
5 m
Splay
0 m
0 m

W
L

Floodplain element

Fl
brs
bgs
Fl
brs

0m — 100m

2 m
0 m

Atkinson Creek, Morrison Formation

L
W

(Coal-prone) floodplain element

Fl
Fr
Fl
C
Fl

0m — 100m

Horse Canyon, Castlegate Sandstone

L
W
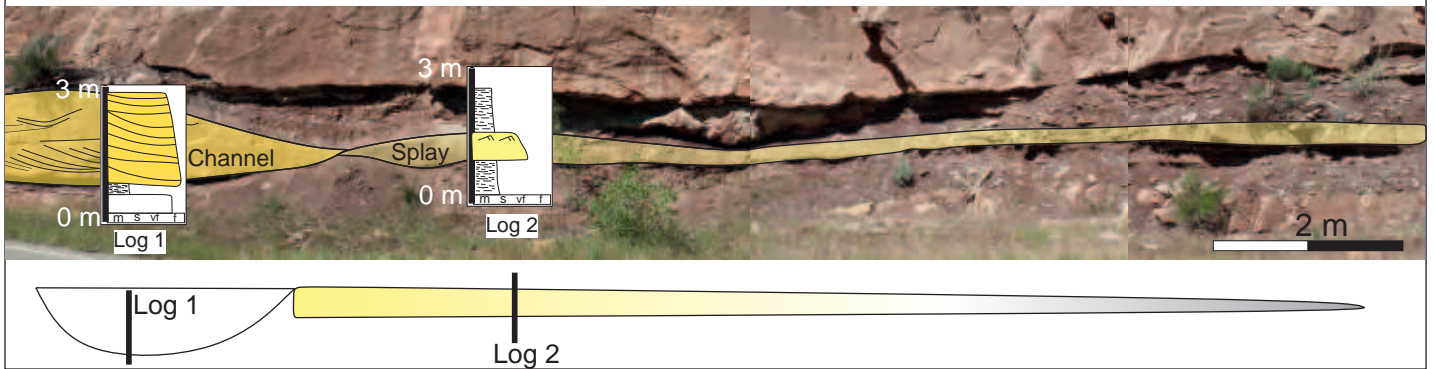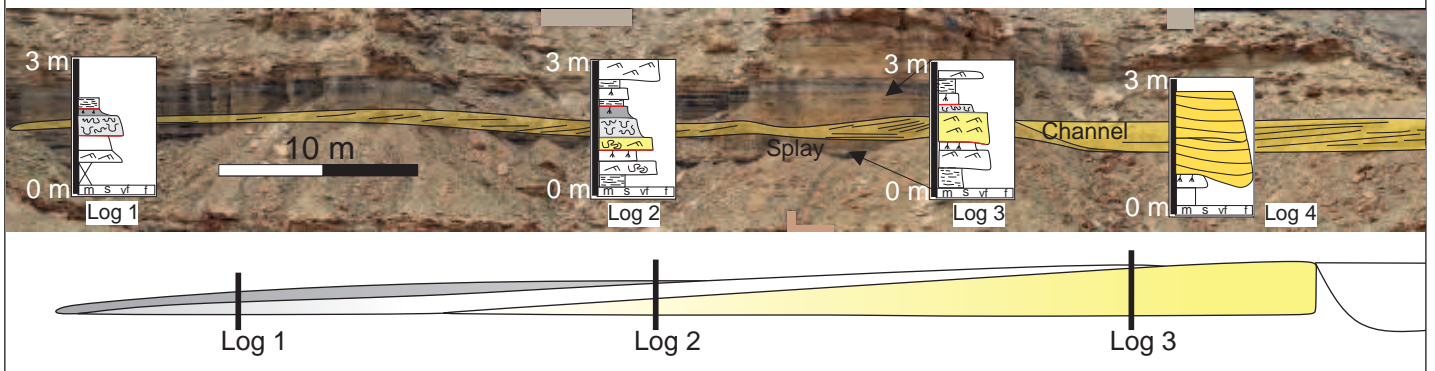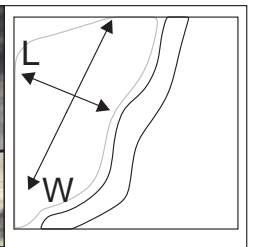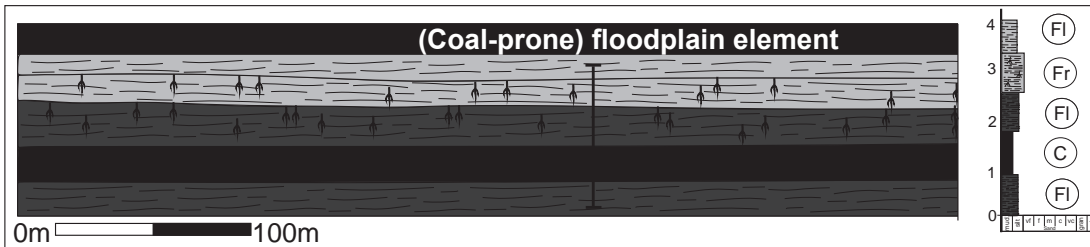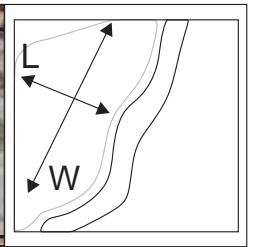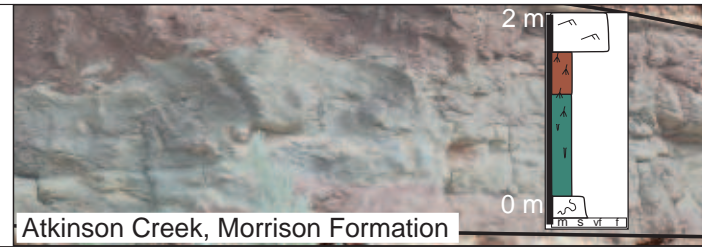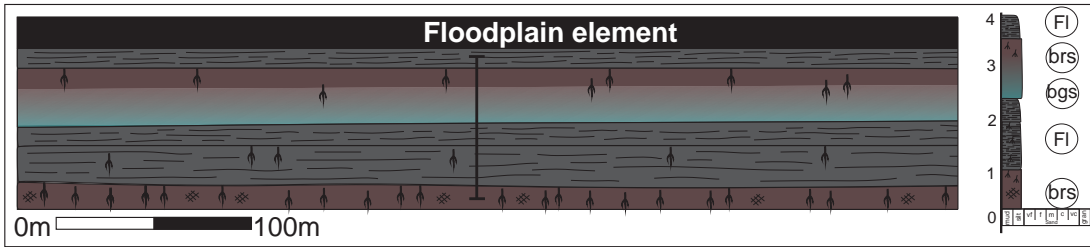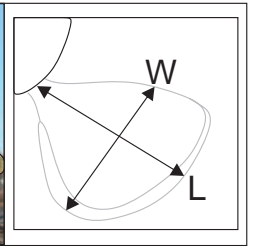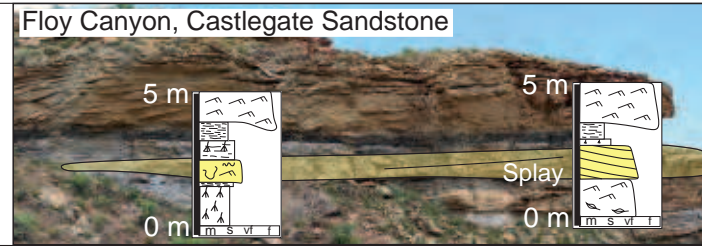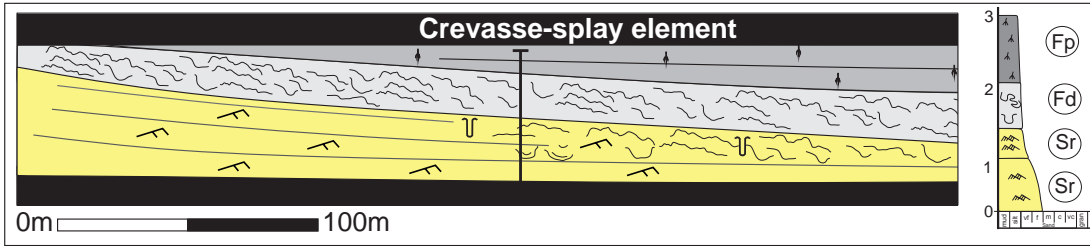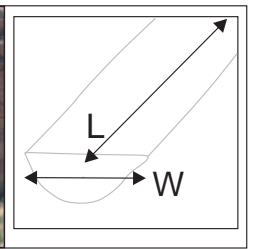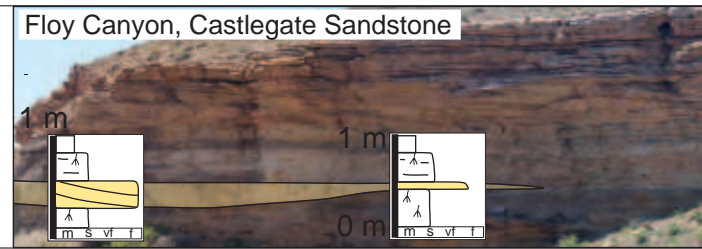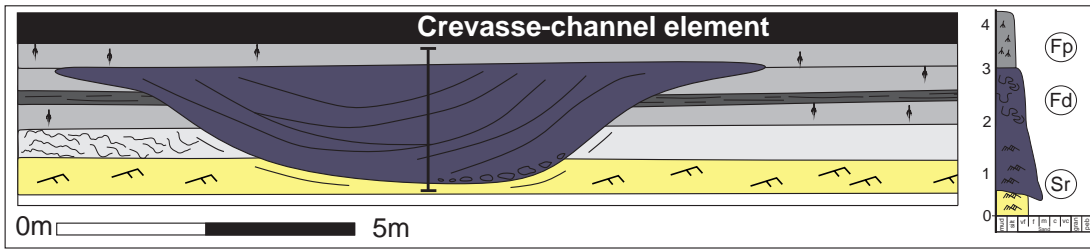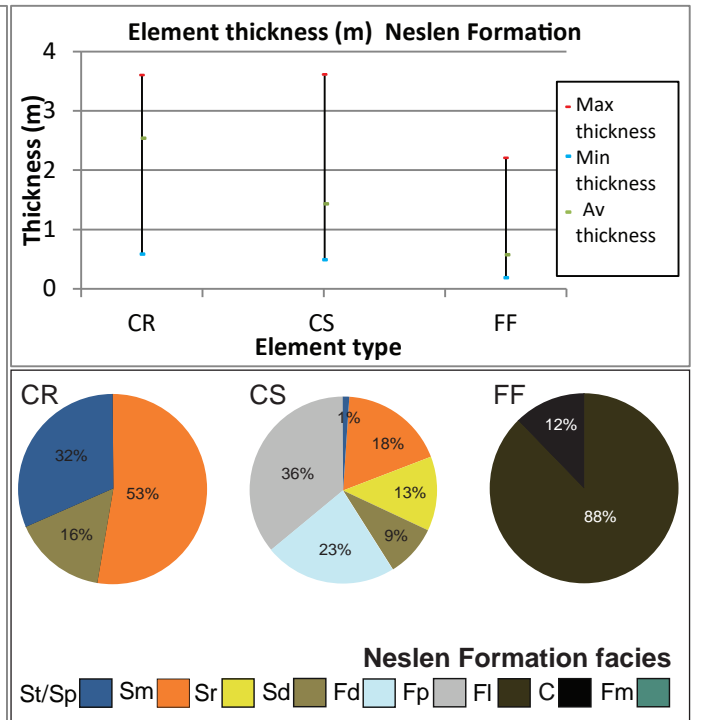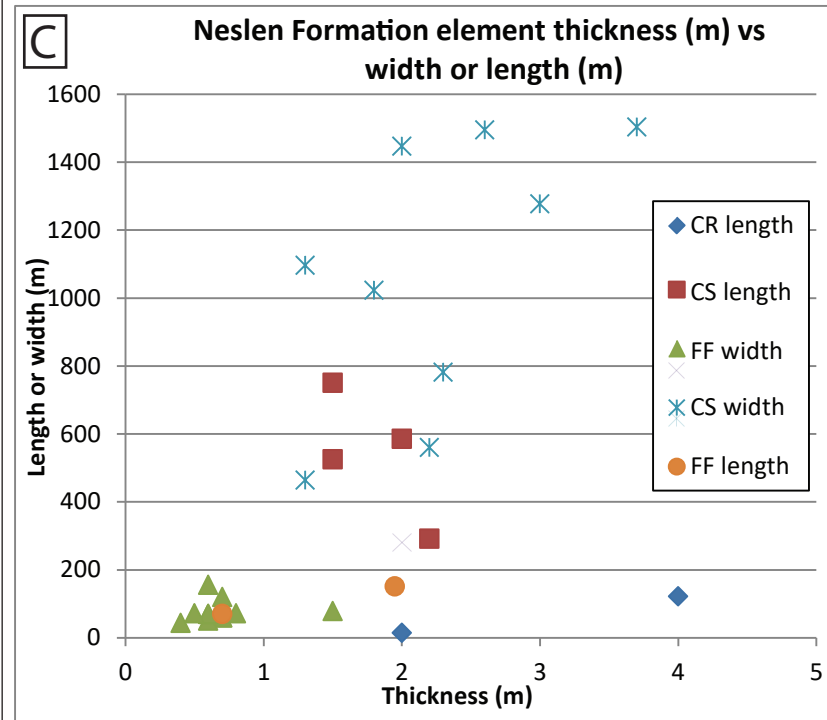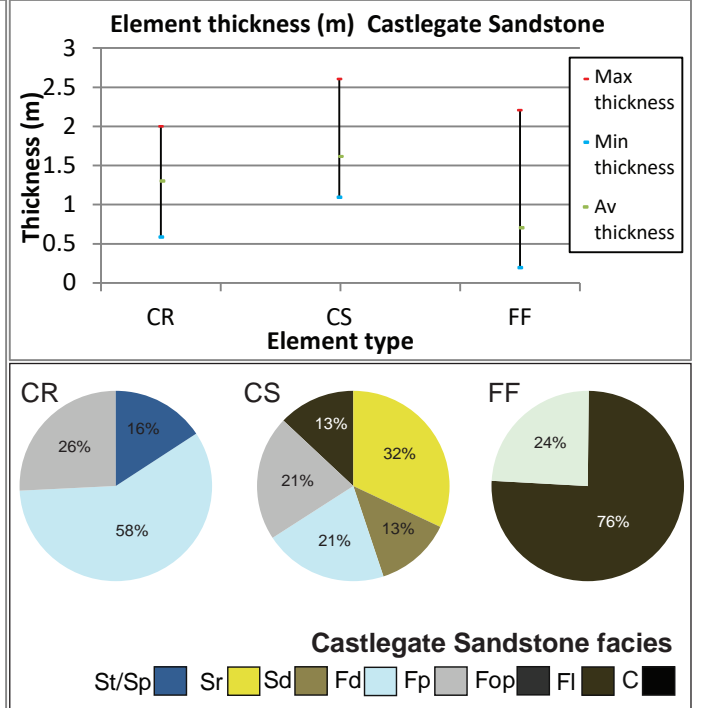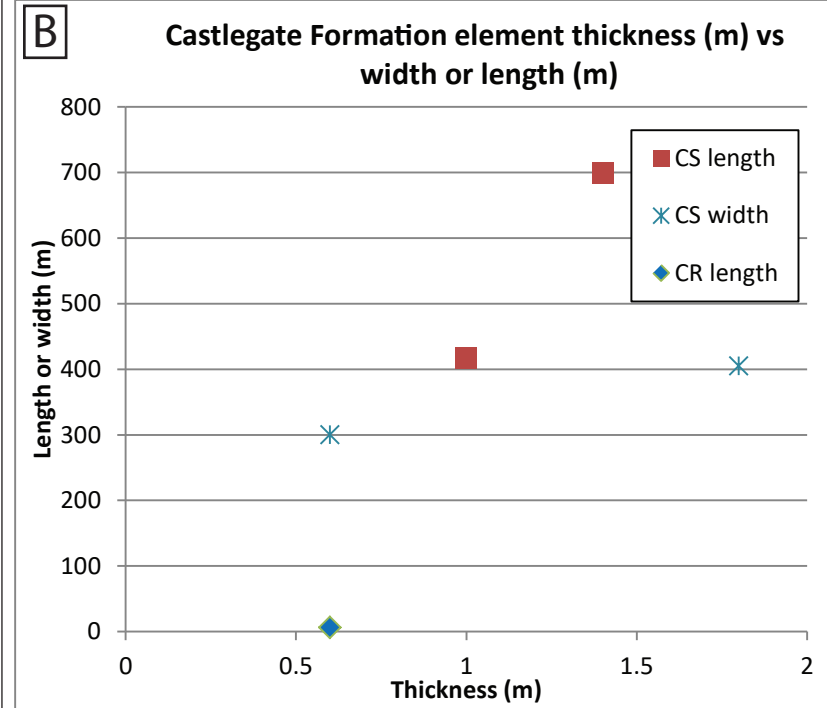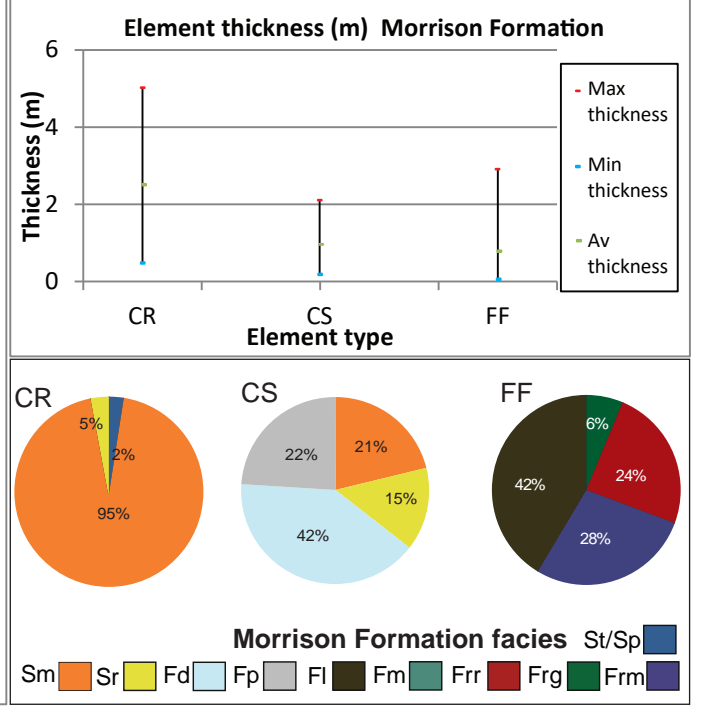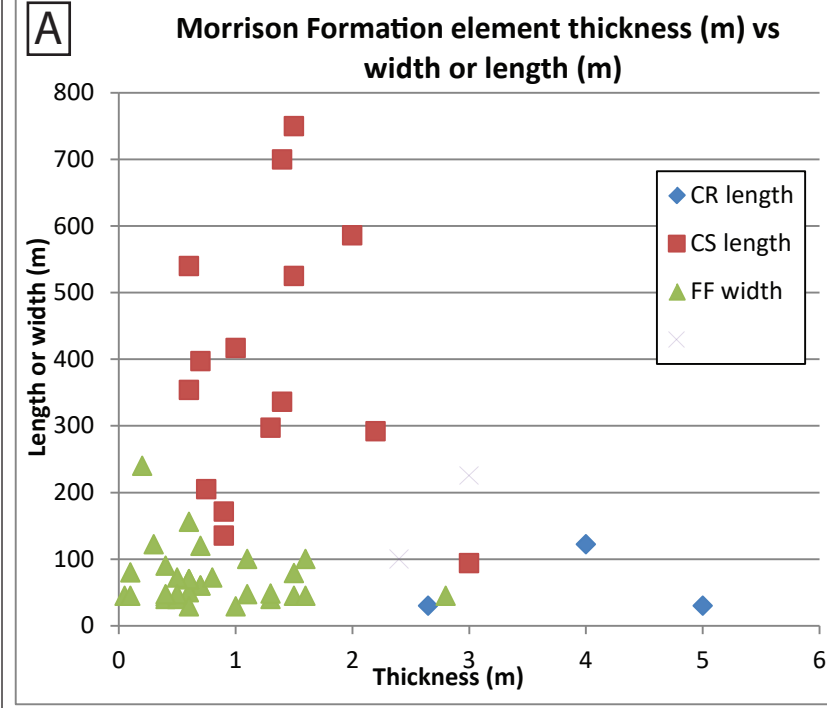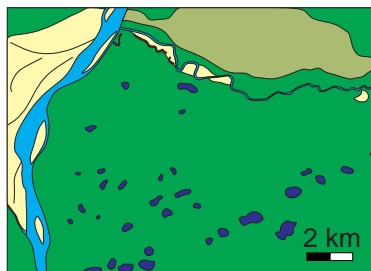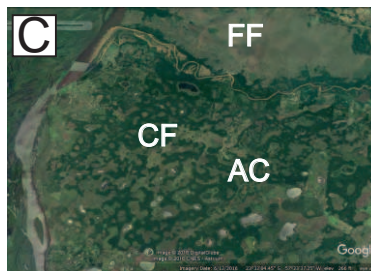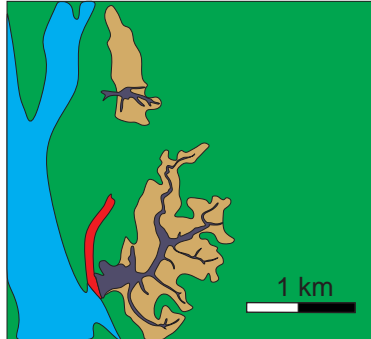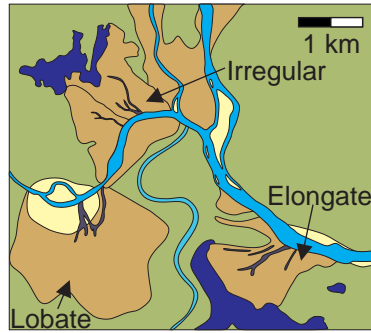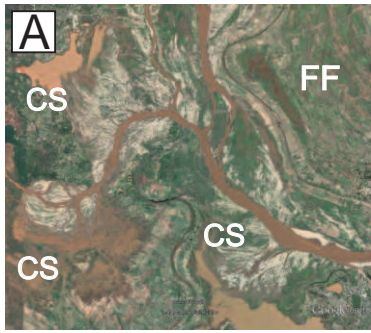
Key

■ Primary Channel	■ Point Bars	■ Secondary Channel	■ Crevasse Splay	■ Tertiary Channel	■ Un-vegetated Floodplain
■ Splay Channel	■ Sparsely Vegetated Floodplain	■ Floodplain Lake	■ Fully Vegetated Floodplain	■ Levees	■ Abandoned Channel

A. Ancient splay body dimensions

Length or width (m) vs Thickness (m)

Legend:
- CS complex Morrison Fm
- CS complex Neslen Fm
- CS element length Morrison Fm
- CS element length Neslen Fm
- CS element length Castegate SST
- CS element width Neslen Fm
- CS element width Castlegate SST
- CS element width Morrison Fm

n=40
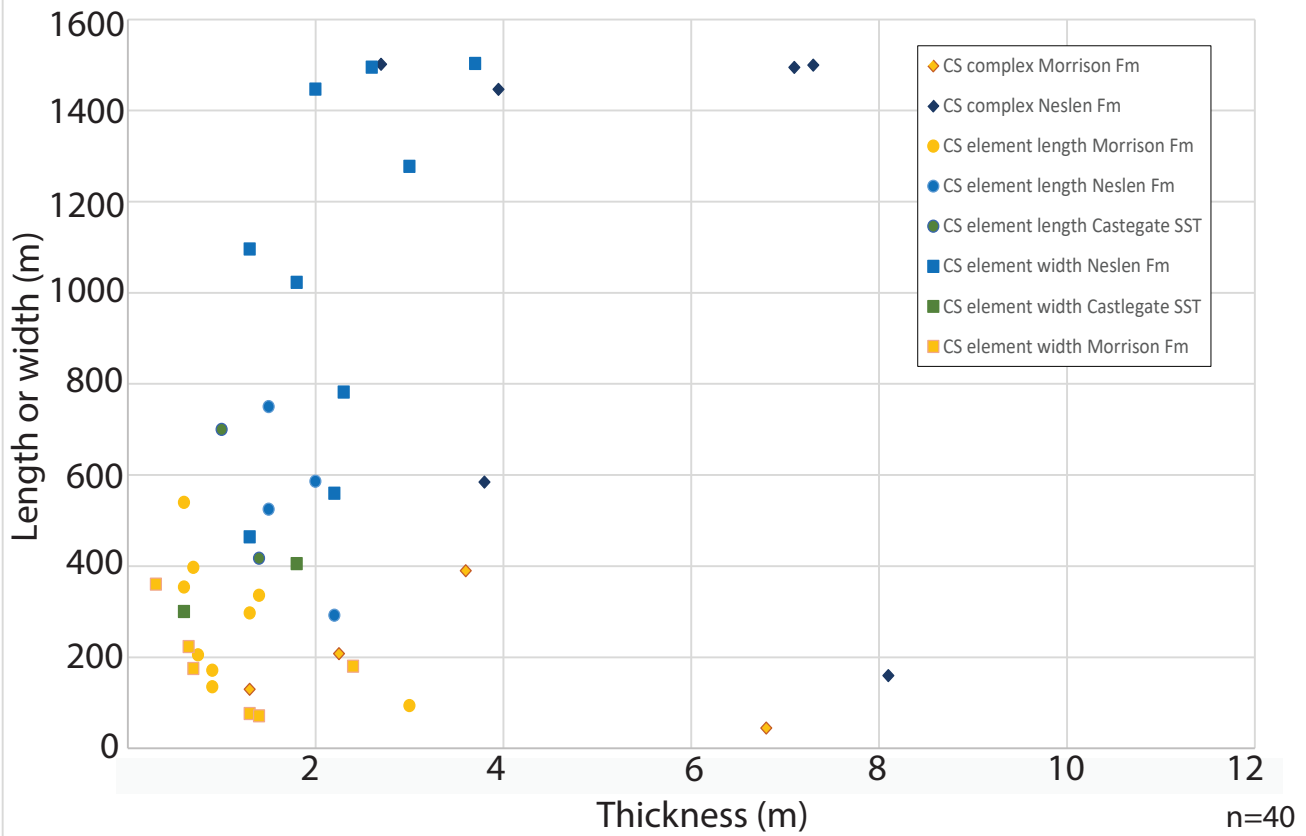
B. Modern splay dimensions

Width (m) vs Length (m)

Legend:
- Helodrano elongate
- Helodrano irregular
- Pilcomayo lobate
- Pilcomayo elongate
- Pilcomayo irregular
- Saskatchewan lobate
- Helodrano lobate
- Saloum lobate
- Saloum elongate
- Saloum irregular
- Mississippi lobate
- Mississippi elongate
- East Madagascar lobate
- East Madagascar elongate

n=122
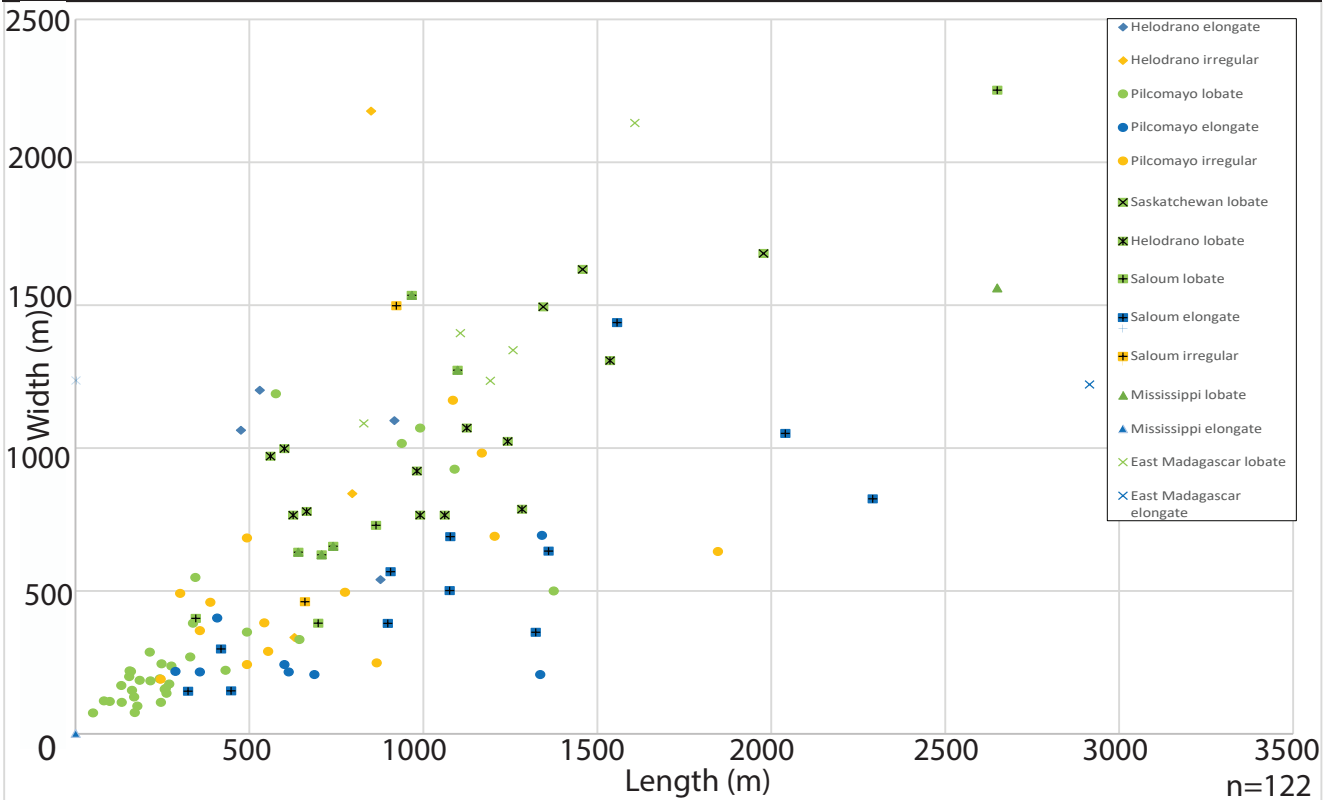
A. Proximal part of crevasse-splay complex
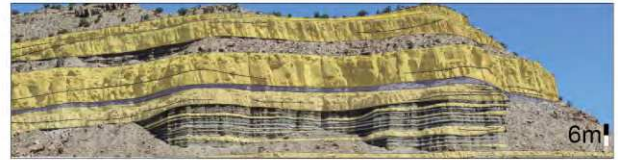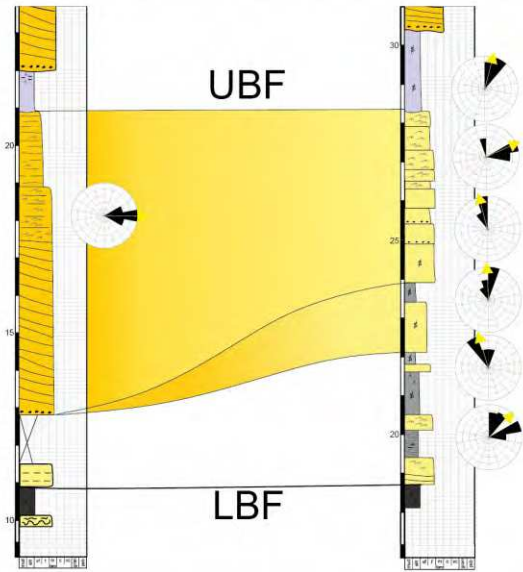
UBF

LBF

6m

2m

B. Medial part of crevasse-splay complex

UBF

LBF

1m

1m

C. Distal part of crevasse-splay complex

UBF

LBF

2m

n=10

n=11

n=9

n=15

n=25
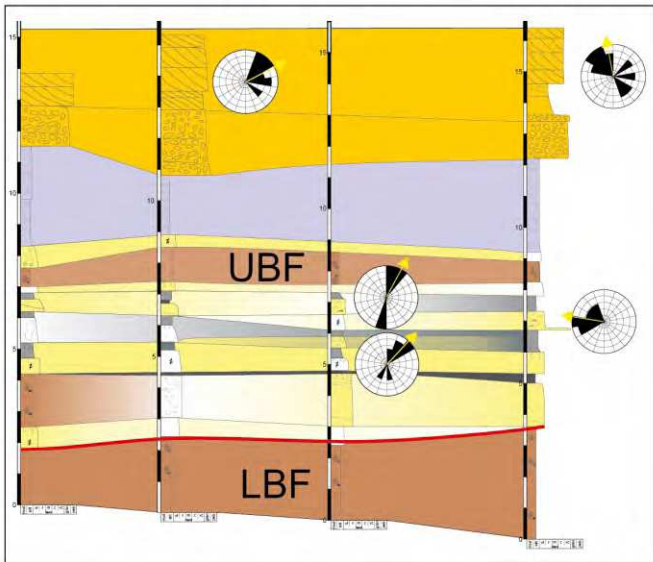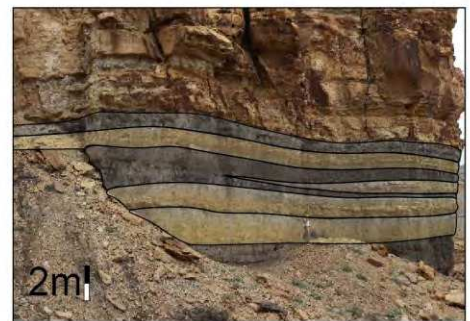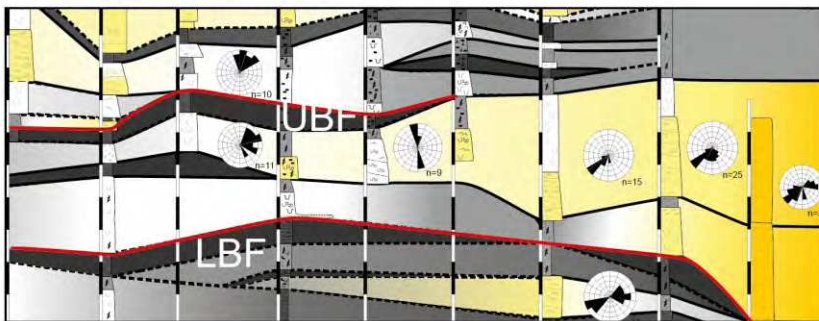
Upper bounding fines= UBF
Lower bounding fines= LBF

Channel

Medial splay

Floodplain

Proximal splay

Distal splay

Floodplain palaeosol

10 m

CH2
C4
B3
CH1
B2
C3
C2
B1
C1
Log 1
Log 2
Log 3

| Splay deposits | Bounding fines e.g. palaeosols |
| Channel deposits | Floodplain fines |
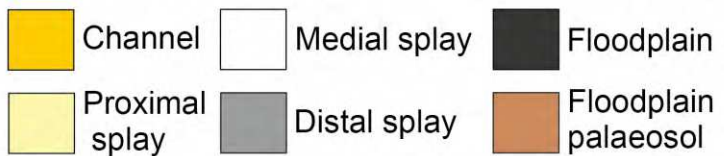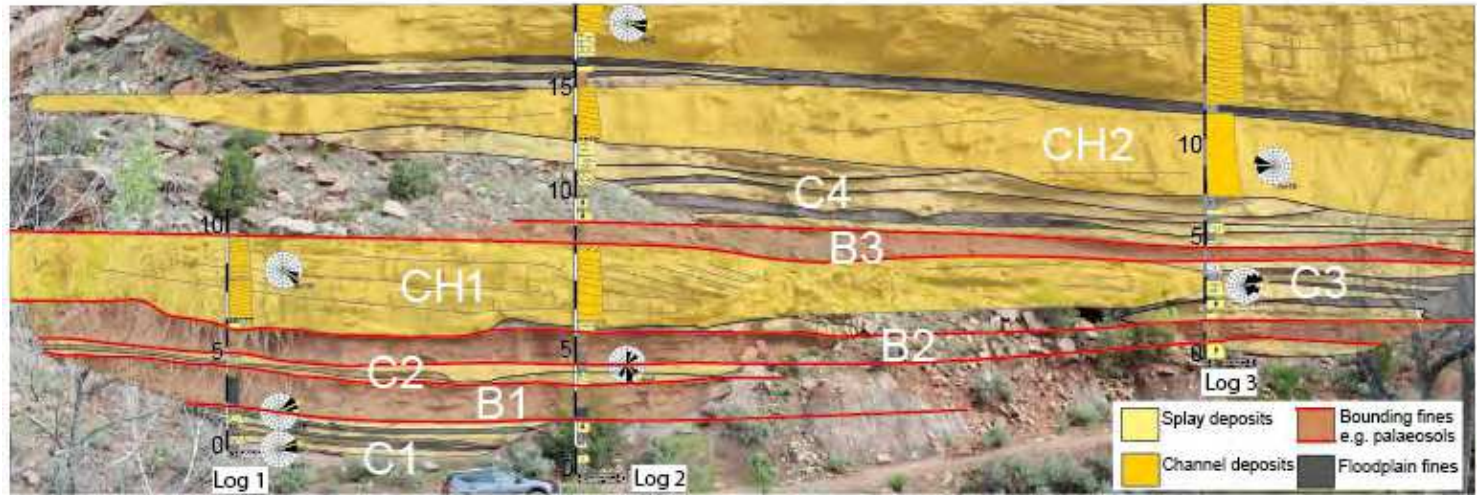
Logged example of a genetically-unrelated splay-elements

Direction of thinning and fining

Orientation NW–SE

50 m

50 m

n≡9

n≡5

n≡13

n≡9

n≡5
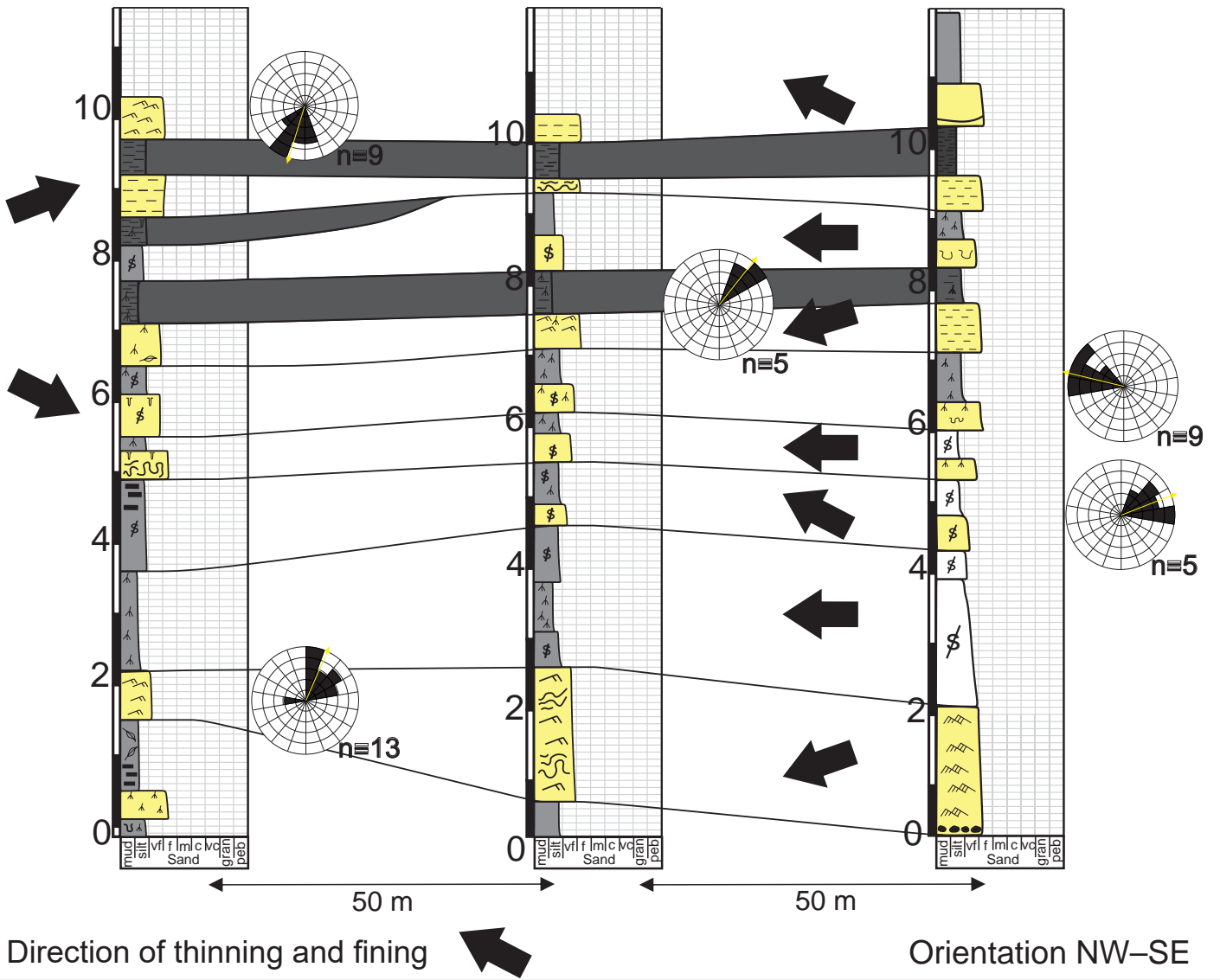
Modern stacked elements within splay complexes

A — inactive crevasse-channels; active crevasse network; 1500m

B — infilled; still active; 500m

C — active crevasse-channels; inactive splay; 500m
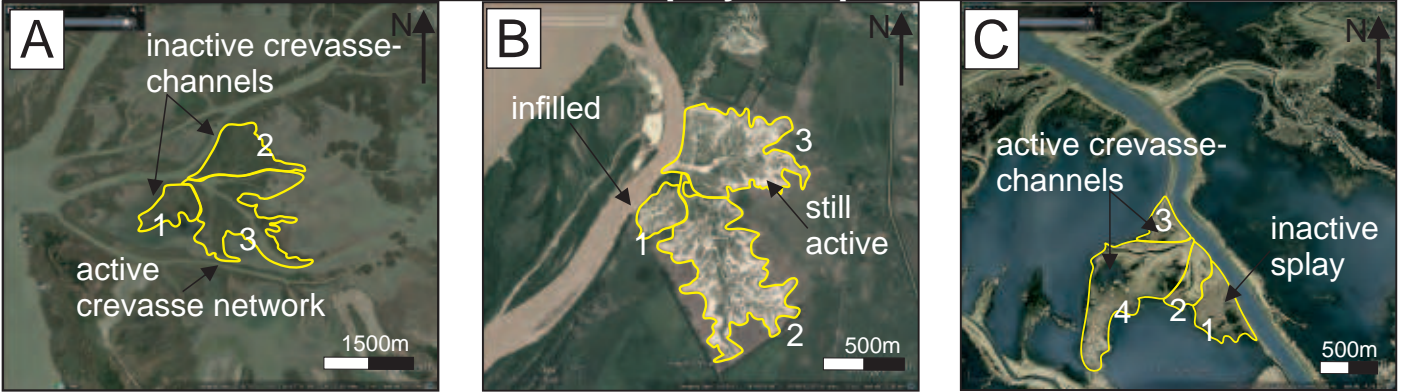
Ancient compensationally stacked elements from the Morrison Formation

D — n=20; n=10; n=4

Legend:
- Splay deposits
- Channel deposits
- Palaeosols
- Floodplain fines

Lateral amalgamation

E — multiple breakout points; merging laterally; 500m

F — well-developed splay laterally amalgamates with smaller splays; different breakouts; 1km

G — Two complexes amalgamate; Two separate breakout points; 700m
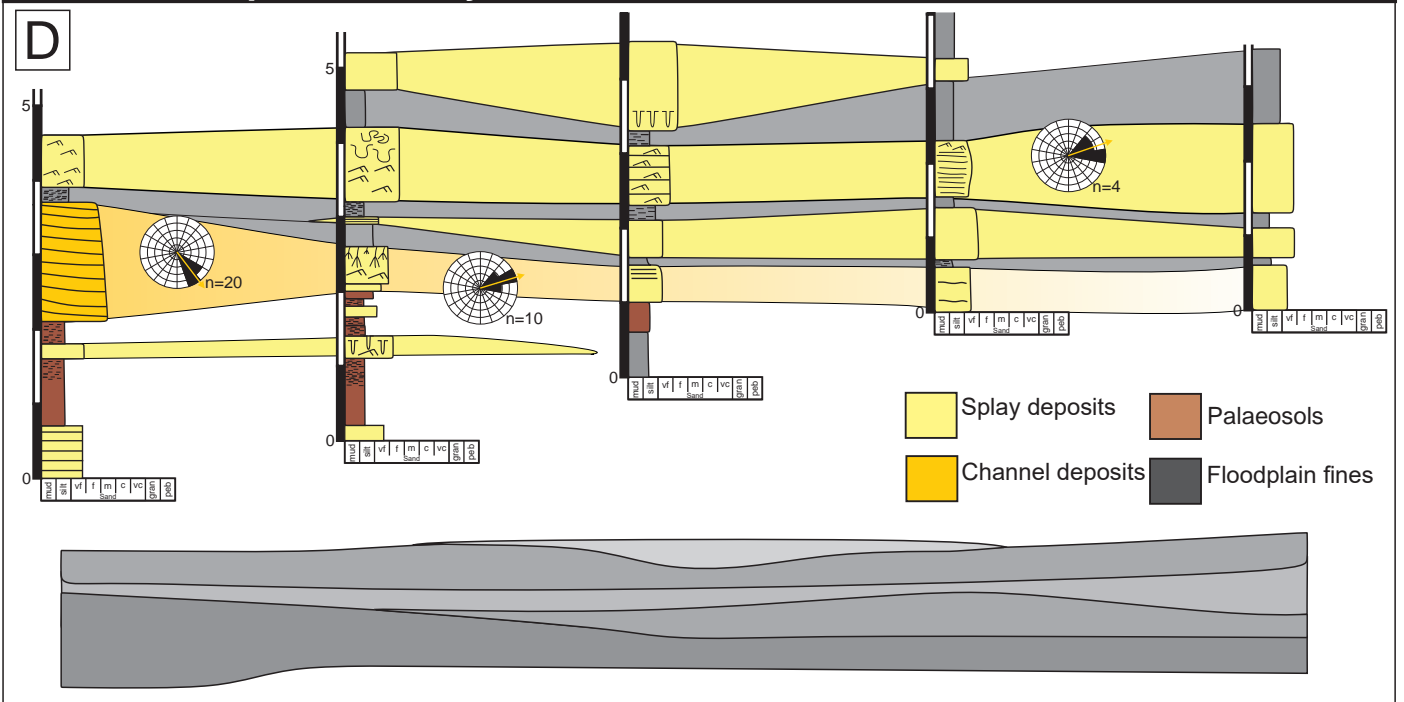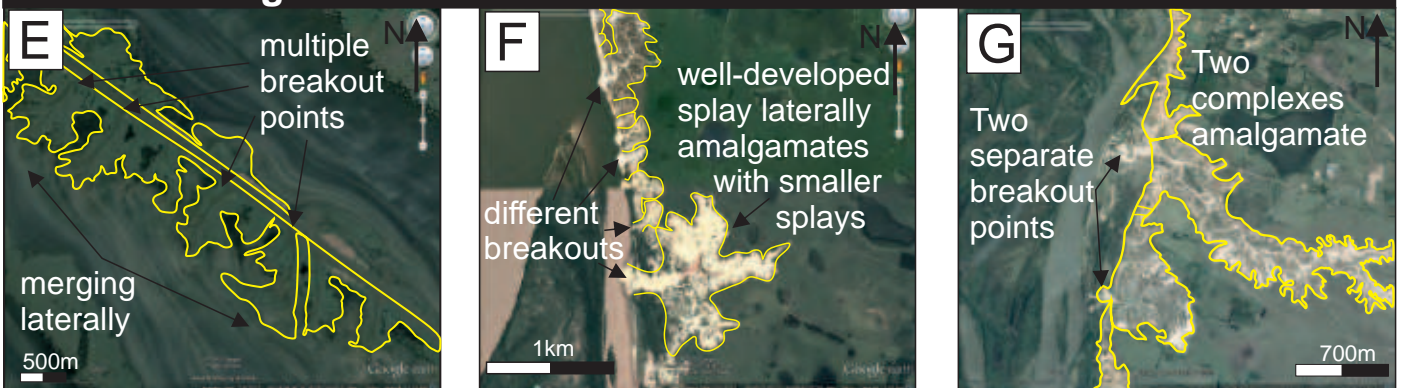
A. Stacking patterns in crevasse-splay complexes

Progradational stacking pattern

Splay-complex

Proximal facies
Proximal facies
Proximal facies

Outline of complex

T1
T2
T3

Splay-complex

Proximal facies
Medial facies
Distal facies

Coarsening and thickening-up

T3
T2
T1

Compensational stacking pattern

Outline of complex

Splay-complex

Distal facies
Medial facies
Proximal facies

Fining and thinning-up

Splay-complex

Proximal facies
Medial facies

Coarsening and thickening-up

T2
T1
T3
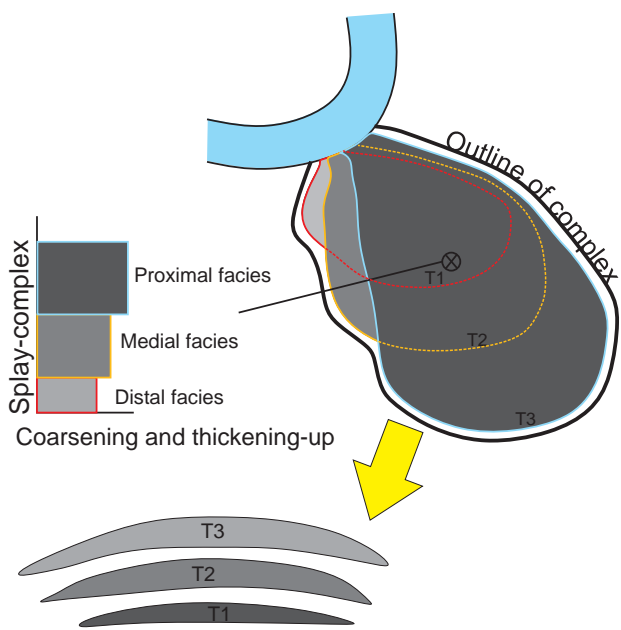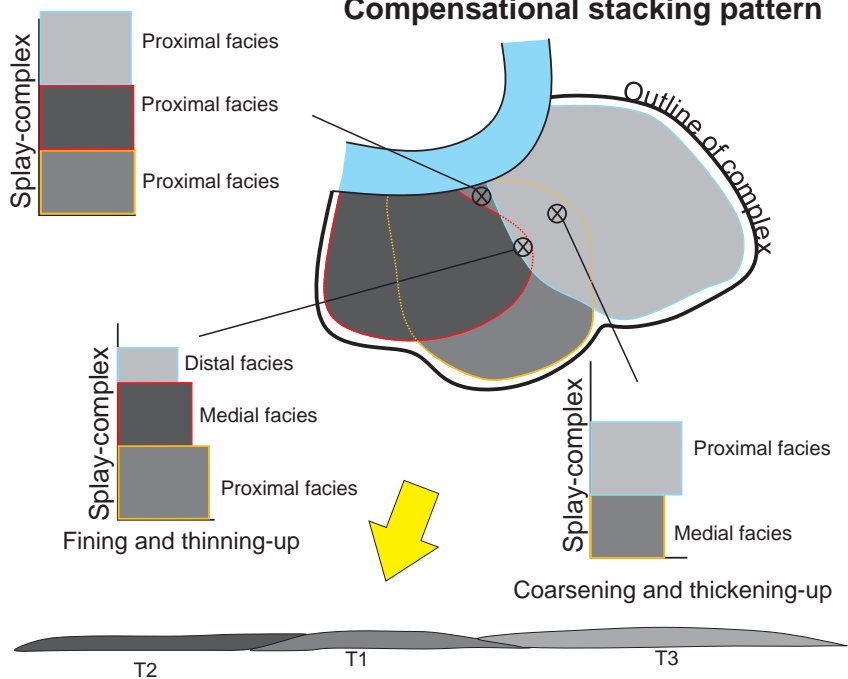
B. Stacking pattern implications

T3
T2
T1
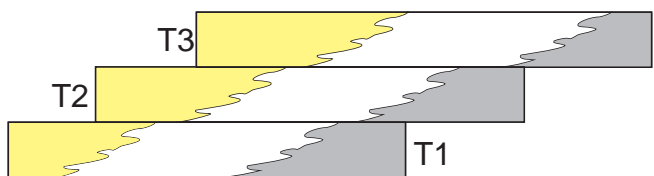
Possible scenario for progradational stacking pattern

T1
T2
T3
Dip orientation

T3
T2
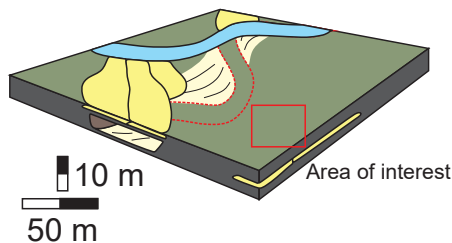T1
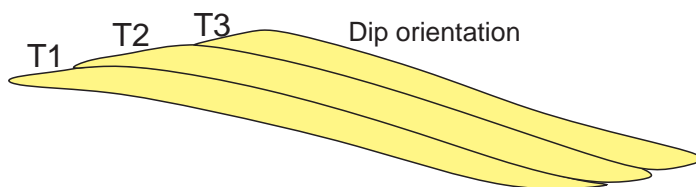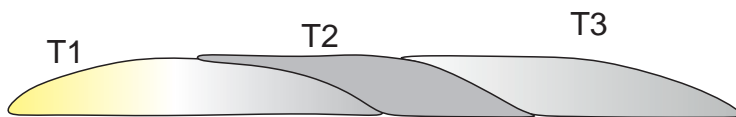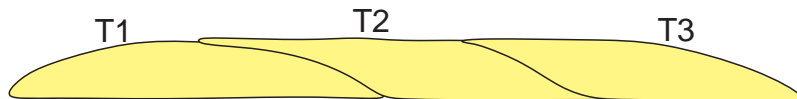
Possible scenarios for compensational stacking pattern

T3
T2
T1

Strike orientation

T1
T2
T3

Strike orientation

T1
T2
T3

C. Longitudinal and lateral merging
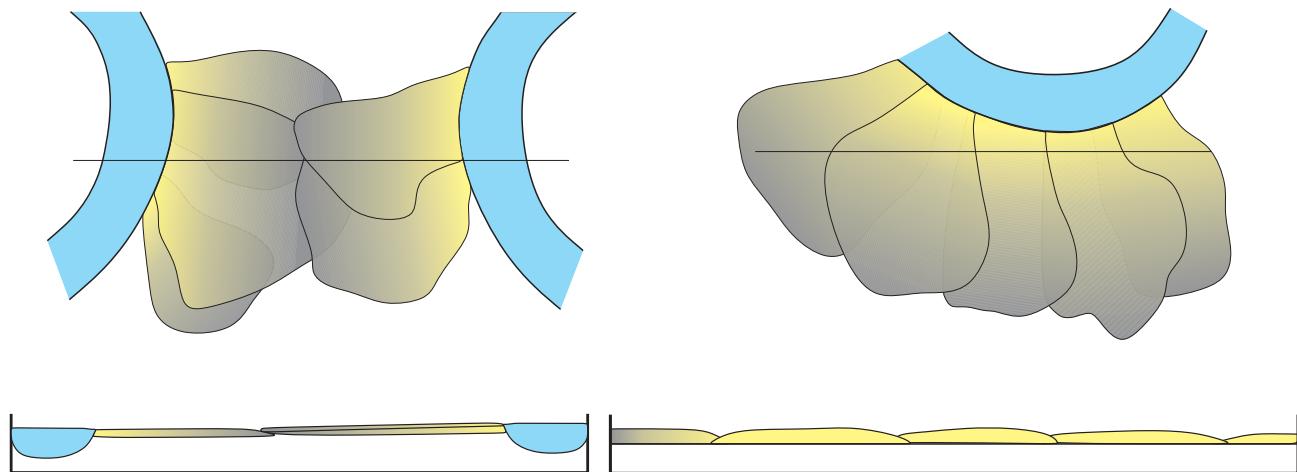
A. Models of floodplain fines and palaeosol deposition

10 m
50 m
Area of interest

Crevasse-splay sedimentation

10 m
50 m
Area of interest
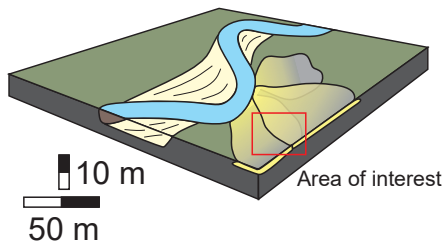
Migration of active channel means slight input of sediment but no crevassing, colonisation of plants
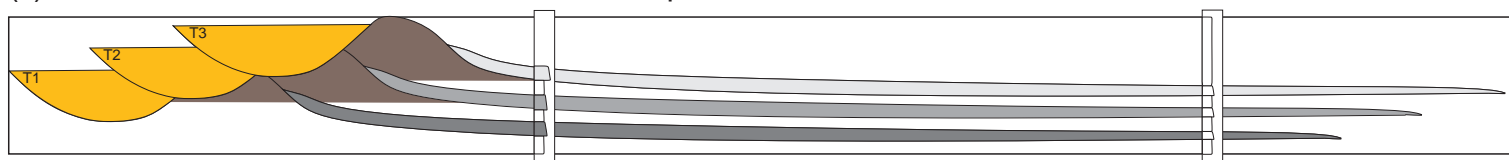
10 m
50 m
Area of interest
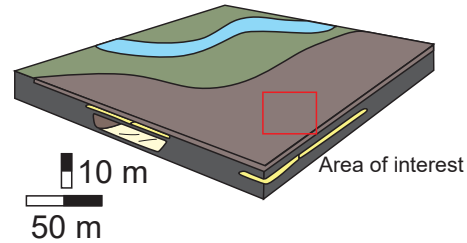
Active channel located far from site of deposition allowing for formation of palaeosols or coals

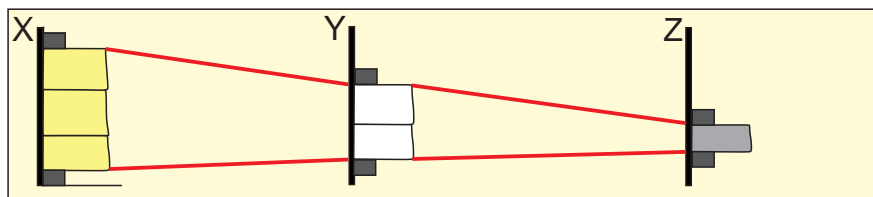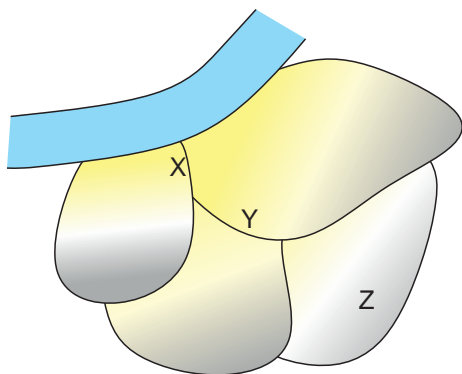**B. Crevasse-splay complexes and crevasse-splay stacks**

(i) Different breakout times; same breakout point

Bankfull level
Floodbasin
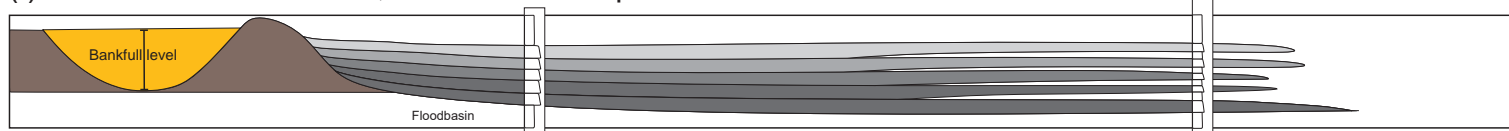
(ii) Different breakout times; different breakout points

T1
T2
T3

C. Crevasse-splay complexes laterally continuity

X
Y
Z

X
Y
Z

Stack of elements as representation of complex

Partial stack of elements as representation of complex

Single element as representation of complex